The STING ligand 2'3'-cGAMP induces an NF-κB-dependent anti-bacterial innate immune response in the starlet sea anemone *Nematostella vectensis*

Shally R. Margolis[1], Peter A. Dietzen[1], Beth M. Hayes[2], Stephen C. Wilson[1,3], Brenna C. Remick[1], Seemay Chou[2,4], Russell E. Vance[1,5,6*]

[1] Division of Immunology and Pathogenesis, Department of Molecular and Cell Biology, University of California, Berkeley, CA 94720 USA
[2] Department of Biochemistry and Biophysics, University of California, San Francisco, San Francisco, CA 94158, USA.
[3] Current Address: Bristol Myers Squibb, 200 Cambridgepark Dr., Cambridge, MA 02140
[4] Chan Zuckerberg Biohub, San Francisco, CA
[5] Cancer Research Laboratory and the Immunotherapeutics and Vaccine Research Initiative, University of California, Berkeley, CA 94720
[6] Howard Hughes Medical Institute, University of California, Berkeley, CA 94720
* correspondence: rvance@berkeley.edu

Author Contributions: S.R.M., P.A.D., B.M.H., S.C.W., S.C. and R.E.V. designed research; S.R.M., P.A.D., B.M.H., S.C.W., and B.C.R. performed research; S.R.M., P.A.D., and B.M.H. analyzed data; S.R.M. and R.E.V. wrote the paper; and P.A.D., B.M.H., S.C.W, and S.C. provided critical review.
Competing Interest Statement: R.E.V. consults for Ventus Therapeutics. The other authors declare no competing interests.
Classification: Biological Sciences; Immunology and Inflammation
Keywords: STING, Cnidaria, *Nematostella vectensis*, NF-κB, innate immunity

Abstract

In mammals, the cGAS-cGAMP-STING pathway is crucial for sensing viral infection and initiating an anti-viral type I interferon response. cGAS and STING are highly conserved genes that originated in bacteria and are present in most animals. By contrast, interferons only emerged in vertebrates; thus, the function of STING in invertebrates is unclear. Here, we use the STING ligand 2'3'-cGAMP to activate immune responses in a model cnidarian invertebrate, the starlet sea anemone *Nematostella vectensis*. Using RNA-Seq, we found that 2'3'-cGAMP induces robust transcription of both anti-viral and anti-bacterial genes, including the conserved transcription factor NF-κB. Knockdown experiments identified a role for NF-κB in specifically inducing anti-bacterial genes downstream of 2'3'-cGAMP, and some of these genes were also found to be induced during *Pseudomonas aeruginosa* infection. Furthermore, we characterized the protein product of one of the putative anti-bacterial genes, the *N. vectensis* homolog of Dae4, and found that it has conserved anti-bacterial activity. This work describes an unexpected role of a cGAMP sensing pathway in anti-bacterial immunity and suggests that a broad transcriptional response is an evolutionarily ancestral output of 2'3'-cGAMP signaling in animals.

Significance statement

Anti-viral immune responses are initiated via signaling pathways such as the STING pathway. In mammals, activation of this pathway results in the production of anti-viral molecules called interferons. Surprisingly, the STING pathway is present in organisms such as sea anemones that lack interferons; the function of this pathway in these organisms is thus unclear. Here we report that in the anemone *Nematostella vectensis,* a small molecule activator of the STING pathway, cGAMP, not only induces an anti-viral response, but also stimulates an anti-bacterial immune response. These results provide insights into the evolutionary origins of innate immunity, and suggest a broader ancestral role for cGAMP-STING signaling that evolved toward more specialized anti-viral functions in mammals.

Introduction

The innate immune system is an evolutionarily ancient system that detects pathogens and initiates their elimination. In mammals, the cGAS-STING pathway is critical for sensing and responding to intracellular DNA, which is particularly important for innate responses to DNA viruses (1, 2). The sensor protein in this pathway, cyclic-GMP-AMP synthase (cGAS), is an enzyme that binds directly to cytosolic DNA and produces 2'3'-cGAMP, a cyclic dinucleotide (CDN) second messenger that binds and activates STING (3-8). Active STING uses its C-terminal tail (CTT) to recruit TBK1, which then phosphorylates and activates the transcription factor IRF3 to induce the expression of type I interferons (IFNs) (9-12). Type I IFNs are secreted cytokines that signal via JAK-STAT signaling to induce transcription of hundreds of anti-viral genes known as interferon-stimulated genes (ISGs) (13, 14). STING also activates NF-κB, MAP kinase (15), STAT6 (16), and autophagy-like pathways (17-20), as well as senescence (21) and cell death (22-26), although the mechanism of activation of these pathways, and their importance during infection, are less well understood.

Type I IFNs are thought to be a relatively recent evolutionary innovation, with identifiable interferon genes found only in vertebrates (27). In contrast, STING and cGAS are conserved in the genomes of most animals and some unicellular choanoflagellates. Remarkably, CDN to STING signaling seems to have originated in bacteria, where it may be important in bacteriophage defense (28, 29). Studies on the function of STING in animals that lack type I IFN have been mostly limited to insects, where STING seems to be protective during viral (30-33), bacterial (34), and microsporidial (35) infection. In insects, STING may promote defense through activation of autophagy (32, 35) and/or induction of NF-κB-dependent defense genes (30, 31, 34); however, the biochemical mechanisms of STING activation in insects remain poorly understood. Biochemically, perhaps the best-characterized invertebrate STING is that of the starlet sea anemone, *Nematostella vectensis,* a member of one of the oldest animal phyla (Cnidaria). *N. vectensis* encodes a surprisingly complex genome that harbors many gene families found in vertebrates but absent in other invertebrates such as *Drosophila* (36). *N. vectensis* STING (nvSTING) and human STING adopt remarkably similar conformations when bound to 2'3'-cGAMP, and nvSTING binds to this ligand with high affinity (K_d < 1nM) (37). The *N. vectensis* genome also encodes a cGAS enzyme that produces 2'3'-cGAMP in mammalian cell culture (17). In vertebrates, STING requires its extended CTT to initiate transcriptional responses (38, 39); however, nvSTING lacks an extended CTT and thus its signaling mechanism and potential for inducing transcriptional responses is unclear. Based on experiments with nvSTING in mammalian cell lines, CTT-independent induction of autophagy has been proposed as the 'ancestral' function of STING (17), but the endogenous function of STING in *N. vectensis* has never been described.

Despite the genomic identification of many predicted innate immune genes (40, 41), few have been functionally characterized in *N. vectensis*. The sole *N. vectensis* Toll-like receptor (TLR) is reported to bind flagellin and activate NF-κB in human cell lines, and is expressed in cnidocytes, the stinging cells that define cnidarians (42). *N. vectensis* NF-κB (nvNF-κB) binds to conserved κB sites, is inhibited by *N. vectensis* IκB (43), and seems to be required for the development of cnidocytes (44). However, no activators of endogenous nvNF-κB have yet been identified. Work probing the putative anti-viral immune response in *N. vectensis* found that double-stranded RNA (dsRNA) injection into *N. vectensis* embryos leads to transcriptional induction of genes involved in the RNAi pathway as well as genes with homology to ISGs (45). This response is partially dependent on a RIG-I-like receptor, indicating deep conservation of anti-viral immunity

(45). However, no anti-viral or anti-bacterial effectors from *N. vectensis* have been functionally tested.

Here, we characterize the response of *N. vectensis* to 2'3'-cGAMP stimulation. Similar to the response of vertebrates to 2'3'-cGAMP, we find robust transcriptional induction of putative anti-viral genes with homology to vertebrate ISGs. In addition, we observed induction of numerous anti-bacterial genes that are not induced during the vertebrate response to 2'3'-cGAMP. We found a selective requirement for nvNF-κB in the induction of some of the anti-bacterial genes, and many of these genes are also induced during *Pseudomonas aeruginosa* infection, suggesting a functional role in anti-bacterial immunity. Of these induced genes, we selected and characterized the anti-bacterial activity of a *Nematostella* domesticated amidase effector (nvDae4), a peptidoglycan cleaving enzyme, and the *Nematostella* LPS- binding protein (nvLBP), a protein that causes membrane permeabilization of *Pseudomonas aeruginosa*. This work demonstrates an evolutionarily ancient role of a cGAMP-sensing pathway in the transcriptional induction of anti-bacterial immunity.

Results

Transcriptional response to 2'3'-cGAMP in Nematostella vectensis

To assess the *in vivo* role of 2'3'-cGAMP signaling in *Nematostella vectensis*, we treated 2-week-old polyps with 2'3'-cGAMP for 24 hours and performed RNA-Seq (Fig. 1A, Fig. S1). Thousands of genes were induced by 2'3'-cGAMP, many of which are homologs of genes known to function in mammalian immunity. Despite the lack of associated gene ontology (GO) terms for many of the differentially regulated genes, unbiased GO term analysis revealed significant enrichment of immune-related terms (Fig. 1B). We confirmed the RNA-Seq results by performing quantitative reverse transcription PCR (qRT-PCR) on 48-hour-embryos treated for 4 hours with 2'3'-cGAMP (Fig. 1C), and found that these genes were also induced at this early developmental stage after a much shorter treatment. We also treated animals with 3'3'-linked cyclic dinucleotides, which are thought to be produced exclusively by bacteria, and which also bind to nvSTING *in vitro*, albeit at lower affinity (37). Both 3'3'-cGAMP and cyclic-di-AMP treatment also induced some smaller number of genes, although all of these genes were induced more strongly by 2'3'-cGAMP (Fig. S1). Interestingly, cyclic-di-GMP treatment led to almost no transcriptional induction, despite having relatively high affinity for nvSTING *in vitro*. This discrepancy may be due to differences in cell permeability among different CDNs, as the ligands were added extracellularly.

Several interesting classes of genes were found to be upregulated in response to 2'3'-cGAMP. For example, several genes involved in the RNAi pathway were induced, including homologs of Argonaute (AGO2), Dicer, and RNA-dependent RNA polymerase (Rdrp1). In addition, many genes that are considered ISGs in mammals were also induced in *N. vectensis*, including Viperin, RNase L, 2'-5'-oligoadenylate synthase (OAS), interferon regulatory factors (IRFs), guanylate-binding proteins (GBPs), and the putative pattern recognition receptors RIG-I-like receptor a (RLRa) and RLRb. These results suggest a conserved role for 2'3'-cGAMP signaling in anti-viral immunity, despite an apparent lack of conservation of type I interferons in *N. vectensis*. Interestingly, we also found that many putative anti-bacterial genes were upregulated in response to 2'3'-cGAMP, including homologs of LPS-binding protein (LBP), lysozyme, perforin-2, Dae4, and mucins. These results indicate that 2'3'-cGAMP stimulation leads to a broad immune response in *N. vectensis*.

To determine whether 2'3'-cGAMP signaled via nvSTING to induce these genes, we injected shRNAs targeting nvSTING into 1-cell embryos and treated with 2'3'-

157 cGAMP 48 hours later. We extracted RNA and performed RNA-Seq on these samples,
158 and surprisingly, while nvSTING transcripts were reduced by ~50%, there was no
159 significant impact on 2'3'-cGAMP-induced gene expression (Fig. S2A, S2B). These
160 negative results were recapitulated in numerous independent qRT-PCR and Nanostring
161 experiments using 9 different shRNAs (3 shown in Fig. S2C). There are several
162 possible explanations for the failure to observe a requirement for nvSTING in 2'3'-
163 cGAMP signaling : (1) a 2-fold reduction in STING transcript levels may not result in a
164 reduction in STING protein levels if the protein is very stable; (2) even if STING protein
165 levels are reduced 2-fold, the reduction may not affect STING signaling due to threshold
166 effects; or (3) nvSTING may not be required for signaling downstream of 2'3'-cGAMP
167 due the presence of a redundant 2'3'-cGAMP sensor in *N. vectensis*. We generated an
168 anti-nvSTING antibody to validate knockdown efficiency at the protein level, but this
169 reagent did not appear to specifically detect nvSTING in anemone lysates. We also
170 tested whether an nvSTING translation-blocking morpholino could inhibit induction of
171 genes in response to 2'3'-cGAMP, but this also had no effect (Fig. S2D). Lastly, we
172 made multiple attempts to generate nvSTING mutant animals using CRISPR, using
173 multiple different guide RNAs, but the inefficiency of CRISPR in this organism and
174 issues with mosaicism prevented the generation of nvSTING null animals. We
175 previously solved the crystal structure of nvSTING bound to 2'3'-cGAMP and showed
176 that binding occurs with high affinity (Kd < 1nM) and in a similar mode as compared to
177 vertebrate STING (37). In addition, we found that when expressed in mammalian cells,
178 nvSTING forms puncta only in the presence of 2'3'-cGAMP, indicating some functional
179 change induced by this ligand (Fig. S2E). Thus, we hypothesize that 2'3'-cGAMP
180 signals via nvSTING, but technical issues and possible redundancy with additional
181 sensors prevent formal experimental evidence for this hypothesis.
182
183 *The N. vectensis NF-κB homolog plays a role in the 2'3'-cGAMP response*
184 We next tested the role of conserved transcription factors that are known to
185 function downstream of STING mammals in the *N. vectensis* response to 2'3'-cGAMP.
186 Interestingly, many of these transcription factors are themselves transcriptionally
187 induced by 2'3'-cGAMP in *N. vectensis* (Fig. 1A). In mammals, the transcription factors
188 IRF3 and IRF7 induce type I IFN downstream of STING activation. While the specific
189 function of these IRFs in interferon induction are thought to have arisen in vertebrates,
190 other IRF family members, with conserved DNA binding residues, are present in *N.*
191 *vectensis* (Fig. S3). We microinjected 1-cell embryos with short hairpin RNAs (shRNAs)
192 targeting each of the 5 nvIRFs or a GFP control, treated with 2'3'-cGAMP, and
193 assessed gene expression by qRT-PCR and/or Nanostring. Knockdown of IRF
194 transcripts by 40-60% did not measurably impact gene induction by 2'3'-cGAMP (Fig.
195 S4). We similarly tested the role of the single *N. vectensis* STAT gene, as mammalian
196 STATs both induce anti-viral genes downstream of Type I IFN signaling, and may even
197 be directly activated by STING (16). Similar to the nvIRFs, we did not observe a
198 significant loss of gene induction by 2'3'-cGAMP in nvSTAT knockdown embryos by
199 both RNA-Seq and Nanostring (Fig. S4). There are several explanations for these
200 findings: (1) sufficient IRF or STAT protein may remain in knockdown animals to
201 transduce the signal, either due to low efficiency of the knockdowns, or to protein
202 stability; (2) the IRFs may act redundantly with each other, and therefore no effect will
203 be seen in single knockdown experiments; or (3) nvIRFs and nvSTAT may not play a
204 role in the response to 2'3'-cGAMP.
205 NF-κB is also known to act downstream of mammalian STING, and appears to
206 be functionally conserved in *N. vectensis* (43). We found that NF-κB signaling

207 components are transcriptionally induced by 2'3'-cGAMP (Fig. 1A). To test the role of
208 nvNF-κB in the 2'3'-cGAMP response, we microinjected embryos with shRNAs targeting
209 nvNF-κB, treated with 2'3'-cGAMP, and performed RNA-Seq (Fig. 2A). 241 genes were
210 transcribed at significantly lower levels in the nvNF-κB knockdown embryos, and of
211 these, 98 were genes induced by 2'3'-cGAMP. Of these genes, 40 are uncharacterized,
212 and no GO terms were significantly enriched (data not shown). Of the induced genes
213 that were annotated in NCBI, we noticed many were homologs of anti-bacterial proteins,
214 including homologs of perforin-2/Mpeg-1, LPS-binding protein (LBP), linear gramicidin
215 synthase, and mucins. We confirmed that 2'3'-cGAMP-mediated induction of these
216 putative anti-bacterial genes was NF-κB dependent by performing qRT-PCR and
217 Nanostring (Fig. 2B; Fig. S5A). Of note, the induction of nvLysozyme was not nvNF-κB
218 dependent (both by RNA-Seq and qRT-PCR; Fig. S5B), indicating either the existence
219 of another pathway for anti-bacterial gene induction, or that our knockdown experiment
220 was not able to affect expression of all nvNF-κB dependent genes. In addition, all of the
221 putative anti-viral genes we examined appeared to be induced independent of nvNF-κB
222 (Fig. S5).
223 We performed BLAST searches of unannotated 2'3'-cGAMP-induced, nvNF-κB-
224 dependent genes and identified several other genes with predicted anti-bacterial
225 activity, including two homologs of bacterial *tae4* genes, and a putative guanylate
226 binding protein (GBP) (*N. vectensis* LOC5515806, hereafter nvGBP-806). The Tae4
227 homologs had been previously identified and will be referred to as nvDae4 proteins
228 (discussed further below; (46)). To confirm the identity of nvGBP-806 as a true GBP
229 homolog, we performed phylogenetic analysis. We identified four conserved *N.*
230 *vectensis* proteins harboring an N-terminal GBP GTPase domain with conserved GBP-
231 specific motifs, including nvGBP-806 (Fig. S6). All of the nvGBP homologs cluster with
232 vertebrate IFN-inducible GBPs and are themselves induced by 2'3'-cGAMP. Finally, we
233 identified several unannotated nvNF-κB dependent, 2'3'-cGAMP-induced genes that
234 appeared to be cnidarian-specific with no identifiable homologs in other animal phyla
235 (Table S1).
236 To test directly whether nvNF-κB is activated in *N. vectensis* upon 2'3'-cGAMP
237 treatment, we treated polyps with cGAMP and performed immunostaining for nvNF-κB
238 (Fig. 2C). Inactive NF-κB is localized to the cytosol, and we observed sparse, cytosolic
239 staining of ectodermal cells in untreated animals, as has been previously reported (43).
240 In contrast, in 2'3'-cGAMP treated animals, we found many more nvNF-κB-positive
241 cells, and in almost all of these, nvNF-κB was found in the nucleus. We performed
242 automated quantification of nuclear nvNF-κB staining, and found that ~3-20% of nuclei
243 captured in our images were positive for nvNF-κB (Fig. 2D). In sum, 2'3'-cGAMP leads
244 to nvNF-κB nuclear localization, and nvNF-κB appears to be required for expression of
245 many putative anti-bacterial, but not anti-viral, genes. Our results demonstrate the first
246 NF-kB agonist in *N. vectensis*, and indicate a conserved immune function for NF-kB in
247 this organism.
248
249 *Gene induction during Pseudomonas aeruginosa challenge*
250 In order to test whether the putative anti-bacterial, NF-κB-dependent genes may
251 indeed be important for anti-bacterial immunity, we tested whether these genes were
252 induced during bacterial challenge of *N. vectensis*. *Pseudomonas aeruginosa* is a
253 pathogenic Gram-negative bacterium that can infect a range of hosts, including plants,
254 mammals, and hydra (47, 48), though infections of *N. vectensis* have not previously
255 been reported. Infection of *N. vectensis* polyps with the *P. aeruginosa* strain PA14 led to
256 polyp death in a dose and temperature dependent manner (Fig. 3A). 48 hours after

infection, we isolated RNA from infected polyps and assayed gene expression. Interestingly, nvSTING expression was induced during PA14 infection (Fig. 3B), and many of the putative anti-bacterial genes we identified as 2'3'-cGAMP-induced were also induced during infection (Fig. 3C). Importantly, PA14 only produces c-di-GMP and not other CDNs. Since c-di-GMP was not sufficient to robustly activate gene expression in *N. vectensis*, we believe that it is likely that the response to PA14 is independent of bacterial CDNs, although we cannot rule out an effect from PA14-produced c-di-GMP. Nevertheless, taken together, these results indicate that the putative anti-bacterial genes we identified as induced by 2'3'-cGAMP are also induced after bacterial challenge.

nvDae4 is a peptidoglycan-cleaving enzyme with anti-bacterial activity

We decided to investigate directly whether some of the genes induced by both 2'3'-cGAMP and bacterial infection are in fact anti-bacterial. Type VI secretion amidase effector (Tae) proteins are bacterial enzymes that are injected into neighboring cells to cleave peptidoglycan, an essential component of bacterial cell walls, leading to rapid cell death (49). While the *tae* genes originated in bacteria, they have been horizontally acquired multiple times in evolution by eukaryotes, and at least one of these so-called “domesticated amidase effectors” (Daes) also has bactericidal activity (46, 50). The *N. vectensis* genome has two *tae4* homologs, both of which were upregulated by 2'3'-cGAMP in an nvNF-κB-dependent manner. However, only one of the *N. vectensis* Dae proteins is predicted to encode a conserved catalytic cysteine (46) required for peptidoglycan hydrolysis. Therefore, we focused our efforts on this homolog, which we call nvDae4 (GI: 5507694). We first tested whether nvDae4 has conserved bactericidal properties by expressing nvDae4 in *E. coli* either with or without a periplasm-targeting signal sequence and measuring bacterial growth (assessed by OD_{600}) over time (Fig. 4A). *E. coli* are Gram-negative bacteria and thus have peptidoglycan compartmentalized within the periplasmic space. Consistent with the predicted peptidoglycan-cleaving function of nvDae4, only periplasmic wild-type (WT) but not catalytic mutant (C63A) nvDae4 expression led to bacterial lysis. In order to test directly whether nvDae4 cleaves peptidoglycan, we produced recombinant protein in insect cells. Since nvDae4 encodes a secretion signal, recombinant nvDae4 was secreted by the insect cells and purified from the cell supernatant. Purified nvDae4 protein was incubated with purified peptidoglycan from either *E. coli* or *Staphylococcus epidermis*. Analysis by high performance liquid chromatography (HPLC) showed that nvDae4 cleaves both Gram-negative (Fig. 4B) and Gram-positive (Fig. S7) derived peptidoglycan. Finally, we wondered whether nvDae4 could directly kill Gram-positive bacteria, as these bacteria contain a peptidoglycan cell wall that is not protected by an outer membrane and is therefore accessible to extracellular factors. We treated *B. subtilis* with recombinant nvDae4 and found that bacteria treated with WT but not C63A nvDae4 protein were killed (Fig. 4C) in a dose-dependent manner (Fig. 4D). Overall these results show that the 2'3'-cGAMP-induced protein nvDae4 is a peptidoglycan-cleaving enzyme with the capacity to kill bacteria.

nvLBP disrupts bacterial membranes

We next wondered whether any of the putative anti-bacterial proteins could directly target Gram-negative bacteria. LPS-binding proteins (LBPs) and bactericidal/permeability-increasing proteins (BPIs) are related, evolutionarily ancient proteins involved in binding, permabilizing, and/or killing Gram-negative bacteria (51). *N. vectensis* has two LBP/BPI homologs, and we focused our efforts on one (GI:

5508577; called nvLBP due to its isoelectric point being more similar to that of human LBP), which we found to be induced by both *P. aeruginosa* infection, and by 2'3'-cGAMP in an nvNF-κB-dependent manner (Fig. 1A, 1C, 2A, 2B, 3C). We purified recombinant nvLBP protein from insect cell supernatants and incubated it with *P. aeruginosa* or *E. coli,* but never saw an impact on bacterial survival (data not shown). We then hypothesized that nvLBP could instead permeabilize outer membranes, which alone might not lead to bacterial lysis, but which might synergize with other anti-bacterial factors during an immune responses (52). To test for membrane permeabilization, we performed 1-*N*-phenylnaphthylamine (NPN) uptake assays with *P. aeruginosa*. NPN fluoresces weakly in aqueous solution but strongly in the presence of phospholipids, which are exposed in Gram-negative bacteria when the outer membrane is disrupted (53). Indeed, in the absence of nvLBP or gentamicin, very little fluorescence was detected; however, upon addition of gentamicin, an antibiotic known to disrupt the Gram-negative outer membrane, or upon addition of nvLBP, we detected a significant increase in fluorescence, indicating that nvLBP does indeed permeabilize *P. aeruginosa* membranes (Figure 4E). Thus, upon 2'3'-cGAMP sensing or *P. aeruginosa* infection, *N. vectensis* produces proteins capable of targeting both Gram-positive and Gram-negative bacteria.

Discussion

In this study, we identified hundreds of *N. vectensis* genes that are induced by the STING ligand 2'3'-cGAMP. Despite over 600 million years of divergence and the absence of interferons, *N. vectensis* responds to 2'3'-cGAMP similarly to mammals by inducing a variety of anti-viral genes. Similarly, Lewandowska et al. (45) reported that *N. vectensis* responds to the synthetic double-stranded RNA poly(I:C), a viral mimic and pathogen-associated molecular pattern (PAMP). In *N. vectensis*, poly(I:C) induced both RNAi pathway components and genes traditionally thought of as vertebrate ISGs. Our combined findings indicate that the pathways linking PAMP detection to ISG expression existed prior to the vertebrate innovation of type I IFNs. Interestingly, some invertebrate species have protein-based anti-viral signaling pathways that perform similar functions to type I IFNs in vertebrates. For example, mosquito cells secrete the peptide Vago upon viral infection, which signals through the JAK-STAT pathway to activate anti-viral immunity (54). Additionally, the oyster *Crassostrea gigas* is thought to have an IFN-like system, but no secreted proteins have yet been identified in this organism (55). *N. vectensis* may also encode an undiscovered IFN-like protein; at a minimum, *N. vectensis* encodes several IRF-like genes (Fig. S3). One attractive hypothesis is that these IRFs are important for the anti-viral response of *N. vectensis*; however, we were unable to see any impact of single knockdown experiments on the induction of genes by 2'3'-cGAMP, though this may be explained by redundancy or technical limitations of our knockdown approach. Nevertheless, an important conclusion of our work is that induction of a broad transcriptional program is an ancestral function of 2'3'-cGAMP signaling, similar to what has been seen in *Drosophila* (31) and choanoflagellates (56). This ancestral transcriptional response complements an additional autophagy response to 2'3'-cGAMP that was previously reported to be induced by nvSTING in mammalian cells (17), and has now also been shown to be induced by 2'3'-cGAMP and STING in choanoflagellates (56).

We found that in addition to an anti-viral response, *N. vectensis* responds to 2'3'-cGAMP by inducing a variety of anti-bacterial genes, including lysozyme, Dae4, perforin-2-like, LPB, and GBPs. With the exception of GBPs, which have dual anti-viral and anti-bacterial activity, these anti-bacterial genes are not induced by 2'3'-cGAMP in

vertebrates; thus, the anti-bacterial response appears to be a unique feature of 2'3'-cGAMP signaling in *N. vectensis*, and it will be interesting to see whether this proves true in other invertebrates, or in additional cell types or contexts in vertebrates. Several of the anti-bacterial genes are also induced by poly(I:C) (45), perhaps indicating a broader anti-pathogen response to PAMPs in *N. vectensis*. Interestingly, we found that nvNF-κB was specifically required for the induction of many of these anti-bacterial genes. This suggests that nvNF-κB activation downstream of 2'3'-cGAMP signaling may have been present in the most recent common ancestor of cnidarian and mammals, and confirms a role for nvNF-κB in *N. vectensis* immunity. Consistent with this speculation, *Drosophila* STING also appears to activate NF-κB (30, 31, 34).

To further establish that 2'3'-cGAMP induces proteins with anti-bacterial activity, we functionally characterized two 2'3'-cGAMP-induced, nvNF-κB-dependent proteins, nvDae4 and nvLBP. We found that nvDae4 is a peptidoglycan-cleaving enzyme with direct bactericidal activity against Gram-positive bacteria. In addition, we found that nvLBP permeabilizes Gram-negative bacterial membranes. Many of the 2'3'-cGAMP-induced NF-κB dependent genes are not recognizable homologs of proteins of known function; thus, they represent good candidates for the discovery of novel anti-bacterial genes in *N. vectensis.*

Using shRNAs to knockdown nvSTING failed to confirm an essential role for nvSTING in the response to 2'3'-cGAMP. However, our previous biochemical and structural studies showed nvSTING binds 2'3'-cGAMP with high affinity (K_d < 1nM) and in a very similar manner as vertebrate STING (37). STING is essential for the response to 2'3'-cGAMP in diverse organisms, including vertebrates, choanoflagellates (56), and insects (31). In addition, nvSTING is highly induced by 2'3'-cGAMP. So despite our negative results, we favor the idea that nvSTING is at least partially responsible for the response of *N. vectensis* to 2'3'-cGAMP. It is possible that *N. vectensis* encodes a redundant 2'3'-cGAMP sensor, but such a sensor would have had to evolve specifically in Cnidarians, or lost independently from choanoflagellates, insects and vertebrates. It is likely that technical limitations of performing shRNA knockdowns in *N. vectensis* accounts for our inability to observe a role for nvSTING in the response to 2'3'-cGAMP, though we cannot exclude the possibility that *N. vectensis* utilizes a distinct 2'3'-cGAMP-sensing pathway.

If indeed 2'3'-cGAMP is signaling via nvSTING, this presents several mechanistic questions. First, in mammals, all known signaling downstream of STING, including NF-κB activation, requires the CTT (38), leading to the question of how invertebrate STING proteins, which lack a discrete CTT, can activate this pathway. Also, nvNF-κB knockdown did not impact the vast majority of 2'3'-cGAMP-induced genes, which may imply the existence of other signaling pathways downstream of nvSTING. How these unidentified pathways become activated is another interesting question and one that could also shed light on mammalian STING signaling. Finally, mammalian STING can also be activated by direct binding to bacterial 3'3'-linked CDNs (57), and nvSTING also binds to these ligands, albeit with lower affinity (37). We found that treatment of *N. vectensis* with these ligands also led to induction of many of the same genes, likely through the same pathway. This perhaps indicates a role for the nvSTING pathway in bacterial sensing, though our preliminary attempts to observe an impact of 2'3'-cGAMP-induced gene expression on bacterial colonization of *N. vectensis* were unsuccessful. Further development of a bacterial infection model for *N. vectensis* will be required to study the anti-bacterial response of this organism *in vivo*.

A crucial remaining question is what activates nvcGAS to produce 2'3'-cGAMP. Double-stranded DNA did not seem to activate this protein in vitro (37), but this could be

due to the absence of cofactors. This protein is also constitutively active when transfected into mammalian cells, but this could be due to overexpression.
Unlike human cGAS, nvcGAS does not have any clear DNA-binding domains, although this does not necessarily exclude DNA as a possible ligand. The *Vibrio* cGAS-like enzyme DncV is regulated by folate-like molecules (58), so there is a diverse range of possible nvcGAS activators. Understanding the role of the cGAS-cGAMP-STING pathway in diverse organisms can shed light on the mechanisms of evolution of viral and bacterial sensing, and on unique ways divergent organisms have evolved to respond to pathogens.

Methods

Nematostella vectensis culture and spawning

N. vectensis adults were a gift from Mark Q. Martindale (University of Florida) and were cultured and spawned as previously described (59). Briefly, animals were kept in 1/3x seawater (12ppt salinity) in the dark at 17°C and fed freshly hatched *Artemia* (Carolina Biological Supply Company) weekly. Spawning was induced every two weeks by placing animals at 23°C under bright light for 8 hours, followed by 2 hours in the dark, and then finally moved to the light where they were monitored for spawning. Egg masses were de-jellied in 4% L-Cysteine (pH 7-7.4) in 1/3x sea water for 10-15 minutes and washed 3 times with 1/3x sea water. Water containing sperm was added to the washed eggs and these were either used immediately for microinjection or allowed to develop at room temperature.

CDN treatment

For the RNA sequencing experiment on polyps (Fig. 1 and Fig. S1), ~4 week old polyps were treated in duplicate in a bath of 500μM c-di-AMP, c-di-GMP, 2'3'-cGAMP, or 3'3'-cGAMP (all InvivoGen) in 1/3x sea water for 24 hours. For remaining cGAMP treatment experiments, 50-100 48-hour old embryos were treated with 100μM 2'3'-cGAMP (InvivoGen) in 1/3x sea water for 4 hours.

RNA sequencing

For the initial CDN treatment experiment using polyps, total RNA was extracted using Qiagen RNeasy Mini kits according to the manufacturer's protocol. Libraries were prepared by the Functional Genomics Laboratory at UC Berkeley using WaferGen PrepX library prep kits with oligo dT beads for mRNA enrichment according to the manufacturer's protocol, and 50 nt single-end sequencing was carried out on the HiSeq4000 (Illumina) by the Vincent J.Coates Genomics Sequencing Laboratory. For all other RNA sequencing experiments on 48 hour embryos, RNA was extracted using Trizol (Thermo Fisher Scientific) according to the manufacturer's protocol. Libraries were prepared by the Functional Genomics Laboratory at UC Berkeley as follows: oligo dT beads from the KAPA mRNA Capture Kit (KK8581) were used for mRNA enrichment; fragmentation, adapter ligation and cDNA synthesis were performed using the KAPA RNA HyperPrep kit (KK8540). Libraries were pooled evenly by molarity and sequenced by the Vincent J.Coates Genomics Sequencing Laboratory on a NovaSeq6000 150PE S4 flowcell (Illumina), generating 25M read pairs per sample. Read quality was assessed using FastQC. Reads were mapped to the *N. vectensis* transcriptome (NCBI: GCF_000209225.1) using kallisto and differential expression was analyzed in R with DESeq2. Differential expression was deemed significant with a $\log_2$ fold change greater than 1 and an adjusted p-value less than 0.05. GO term analysis

457 was performed using goseq with GO annotations from
458 https://figshare.com/articles/dataset/Nematostella_vectensis_transcriptome_and_gene_
459 models_v2_0/807696. The EnhancedVolcano package
460 (https://github.com/kevinblighe/EnhancedVolcano) was used to generate volcano plots.
461 Heatmaps are based on regularized log-transformed normalized counts and Z-scores
462 are scaled by row. All RNA-Seq results can be found in Supplementary File S1.
463
464 **Quantitative Real-Time PCR (qRT-PCR)**
465 Embryos and polyps were lysed in TRIzol (Invitrogen) and RNA was extracted
466 according to the manufacturer's protocol. 500ng of RNA was treated with RQ1 RNase-
467 free DNase (Promega) for and reverse transcribed with Superscript III (Invitrogen).
468 Quantitative PCR was performed using SYBR Green (Thermo Fisher Scientific) with 0.8
469 μM of forward and reverse primers on a QuantStudio 5 Real-Time PCR System
470 (Applied Biosystems) with the following cycling conditions: 50°C 2 min; 95°C 10 min;
471 [95°C 15 sec, 60°C 1 min] x 40; 95°C 15 sec; 60°C 1 min; melt curve: step 0.075 °C/s to
472 95°C. Fold changes in expression levels were normalized to actin and calculated using
473 the $2^{-\Delta\Delta Ct}$ method. Student's t-tests were performed on ΔCt values. All primer sequences
474 used in this study can be found in Supplementary File S2.
475
476 **shRNA microinjection**
477 Short hairpin RNAs for microinjection were prepared by *in vitro* transcription as
478 previously described (60). Briefly, unique 19 nucleotide targeting motifs were identified
479 and used to create oligonucleotides with the following sequence: T7 promoter—19nt
480 motif—linker—antisense 19nt motif–TT. RNA secondary structure was visualized using
481 mfold (http://www.unafold.org/mfold/applications/rna-folding-form.php) to ensure a
482 single RNA conformation. Both sense and anti-sense oligonucleotides were synthesized
483 and mixed to a final concentration of 25μM, heated to 98°C for 5 minutes and cooled to
484 24°C before use as template for *in vitro* transcription using the Ampliscribe T7-Flash
485 Transcription Kit (Lucigen). Reactions were allowed to proceed overnight, followed by a
486 15 minute treatment with DNase and subsequent purification with Direct-zol™ RNA
487 MiniPrep Plus (Zymo Research). All shRNAs used in this study can be found in
488 Supplementary File S2.
489 Microinjections of one-cell embryos were carried out as previously described
490 (61). shRNAs were diluted to a concentration of 500-900 ng/μl (ideal concentrations
491 were determined experimentally) in RNase-free water with fluorescent dextran for
492 visualization. Injected embryos were monitored for gross normal development at room
493 temperature and used for experiments 48 hours later unless otherwise indicated.
494 Knockdowns for each gene were performed using at least two different shRNAs and
495 phenotypes were confirmed in at least 3 independent experiments.
496
497 **Immunohistochemistry, imaging, and quantification**
498 Polyps treated for 4 hours with 100μM 2'3'-cGAMP were stained for nvNF-κB as
499 previously described (62). Briefly, polyps were fixed in 4% paraformaldehyde in 1/3x
500 sea water overnight at 4°C with rocking, and subsequently washed 3 times with wash
501 buffer (1× PBS, 0.2% Triton X-100). Antigen retrieval was performed by placing
502 anemones in 95°C 5% urea for 5 minutes and allowing them to cool to room
503 temperature before washing 3 times in wash buffer. Samples were blocked overnight at
504 4°C in blocking buffer (1× PBS, 5% normal goat serum, 1% bovine serum albumin,
505 0.2% Triton X-100). Samples were stained with anti-nvNF-κB (1:100; gift of Thomas
506 Gilmore, Boston University) in blocking buffer for 90 minutes at room temperature and

507 washed 4 times in wash buffer. Samples were then incubated in FITC-anti-Rabbit IgG
508 (1:160; F9887, Sigma-Aldrich) in blocking buffer for 90 minutes at 37°C. Finally,
509 samples were washed in wash buffer, stained with 1 μg/mL of DAPI for 10 minutes,
510 washed again, and mounted in Vectashield HardSet Mounting medium and imaged on a
511 Zeiss LSM 710 AxioObserver. Imaris 9.2 (Bitplane) was used to create 3D surfaces
512 based on DAPI expression, and surface statistics were exported and analyzed in
513 FlowJo (BD) to quantify nuclear nvNF-κB expression as previously described (63).
514
515 **Bacterial infection**
516 Single colonies of *Pseudomonas aeruginosa* strain PA14-GFP were cultured
517 overnight in LB with 50μg/ml of carbenicillin, centrifuged for 5 minutes at 3000 x *g,*
518 resuspended to an OD_{600} of 0.1, 0.01, or 0.001 in 1/3x sea water and used to infect
519 polyps, which were kept at room temperature or 28°C as indicated. Inputs were plated
520 to calculate CFU/ml. Polyp survival was monitored daily. For expression analysis,
521 polyps were homogenized in Trizol and RNA extraction and qPCR were performed as
522 indicated above.
523
524 **Protein purification**
525 Double-stranded DNA encoding codon optimized nvLBP lacking its signal
526 peptide was ordered from IDT, and nvDae4 lacking its signal peptide was cloned from
527 cDNA. These fragments were then cloned into the pAcGP67-A baculovirus transfer
528 vector for secreted, His-tagged protein expression. The plasmid for expressing mutant
529 nvDae4 (C63A) was made from the pAcGP67-A-nvDae4 plasmid using Q5 site-directed
530 mutagenesis (NEB) according to the manufactures protocol. Plasmids were transfected
531 into Sf9 insect cells ($2x10^6$ cells/ml in 2ml) using Cellfectin II Reagent (Gibco) along with
532 BestBac 2.0 v-cath/chiA Deleted Linearized Baculovirus DNA (Expression Systems) for
533 6 hours, after which media was replaced and cells were left for 1 week at 25°C.
534 Supernatants were harvested and 50 µL were used to infect $7x10^6$ Sf9 cells in 10ml of
535 media for 1 week at 25°C. Supernatants containing secondary virus were harvested,
536 tested, and used to infect High Five cells (2 L at $1.5x10^6$ cells/ml) for 72 hours at 25°C
537 with shaking. Supernatants containing protein were harvested by centrifuging for 15 min
538 at 600 x *g* at 4°C and subsequently passing through a 0.45 µm filter to remove all cells.
539 Supernatants were buffered to 1x HBS (20mM HEPES pH 7.2, 150mM NaCl), mixed
540 with 2 mL of Ni-NTA agarose were per liter, and rotated at 4°C for 2 hours. Ni-NTA
541 resins with bound protein were collected on a column by gravity-flow and washed with
542 30x column volume of wash buffer (for nvDae4: 20mM HEPES, 1M NaCl, 30mM
543 imidazole, 10% glycerol; for nvLBP: 20mM HEPES, 400mM NaCl, 20mM imidazole).
544 Protein was eluted in 1 mL fractions using 1xHBS supplemented with 200mM imidazole.
545 Buffer was exchanged to 1xHBS+ 2mM DTT using Econo-Pac10DG Desalting
546 Prepacked Gravity Flow Columns (Bio-rad) according to the manufacturers protocol,
547 and proteins were concentrated using 10kDa (for nvDae4) or 30kDa (for nvLBP)
548 concentrators (Millipore).
549
550 **Bacterial killing assays**
551 For expression in *E. coli*, nvDae4 WT and C63A lacking the endogenous signal
552 sequence were cloned into the pET28a vector for inducible cytosolic expression, or the
553 pET22b vector for inducible periplasmic expression. *E. coli* (BL21 DE3 strain) were
554 freshly transformed with the vectors and grown overnight in LB with 50 µg/mL
555 carbenicillin shaking at 37°C. Overnight cultures were backdiluted in LB to the same

556 OD_{600} and grown to log phase before induction with 0.25mM IPTG. Plates were kept
557 shaking at 37°C and OD_{600} was read every 5 minutes for 3 hours.
558 *Bacillus subtilis*-GFP (derivative of strain 168; BGSC accession #1A1139) was
559 grown to log-phase in LB with 100 µg/mL spectinomycin, centrifuged, resuspended in
560 0.5xHBS, and incubated alone or with nvDae4 WT or C63A at indicated concentrations
561 for 2-3 hours at 37°C. Serial dilutions were plated on LB agar with 100 µg/mL
562 spectinomycin to determine CFU.
563
564 **Peptidoglycan cleavage assays**
565 Peptidoglycan (PG) was purified and analyzed as previously described (50).
566 Briefly, *Escherichia coli* BW11325 (from Carol Gross, UCSF) and *Staphylococcus*
567 *epidermis* BCM060 (from Tiffany Scharschmidt, UCSF) were grown to an OD600 of 0.6,
568 harvested by centrifugation, and boiled in SDS (4 % final concentration) for 4 hours with
569 stirring. After washing in purified water to remove SDS, the peptidoglycan was treated
570 with Pronase E for 2 h at 60°C (0.1 mg/ml final concentration in 10 mM Tris-HCl pH7.2
571 and 0.06 % NaCl; pre-activated for 2 h at 60 °C). Pronase E was heat inactivated at
572 100°C for 10 min and washed with sterile filtered water (5 x 20 min at 21k × *g*). PG from
573 Gram-positive bacteria (*Se*) was also treated with 48% HF at 37°C for 48 h to remove
574 teichoic acids, followed by washes with sterile filtered water. nvDae4 enzyme (WT and
575 C63A) was added (1-10 µM in 10 mM Tris-HCl pH 7.2 and 0.06% NaCl) and incubated
576 O/N at 37°C. Enzymes were heat inactivated at 100°C for 10 min. Mutanolysin (Sigma
577 M9901, final concentration 20 µg/ml) was added to the purified peptidoglycan and
578 incubated overnight at 37 °C. The peptidoglycan fragments were reduced, acidified,
579 analyzed via HPLC (0.5 ml/min flow rate, 55°C with Hypersil ODS C18 HPLC column,
580 Thermo Scientific, catalog number: 30103-254630).
581
582 **NPN uptake assay**
583 PA14-GFP cultures were grown from a single colony for 8 hours shaking at 37°C,
584 then 500µL were used to inoculate a 50 mL culture overnight. 25 mL of culture were
585 centrifuged at 600 x *g* for 10 minutes and resuspended in 1 M HEPES to an OD_{600} of
586 0.2-0.4. 96 µL of PA14 culture were added to the wells of a blacked-walled 96-well plate
587 along with 2 µL of 500 µM *N*-Phenyl-1-naphthylamine (NPN; Sigma-Aldrich) in acetone
588 or acetone alone. Baseline fluorescence was read every 30 seconds on a Spark
589 microplate reader (Tecan) with the following conditions: 350nm excitation; 420nm
590 emission; manual gain 70%. After 10 minutes, 2 µL of buffer, gentamycin (final
591 concentration 20 µg/mL), or LBP (final concentration 4.6 µM) were added to triplicate
592 wells and fluorescence was read for 20 minutes. Values were normalized to relevant
593 reaction wells without NPN and plotted.
594
595 ***Supplemental methods***
596
597 **Phylogenetic analysis**
598 Protein sequences containing domains of interest were downloaded from NCBI,
599 with the exception of nvGBP6 and nvGBP7, for which RNA-seq data showed additional
600 nucleotide usage relative to the reference sequence (all sequences can be found in
601 Supplementary File S2). These were aligned using on phylogeny.fr using MUSCLE and
602 manipulated in Geneious. For the GBP and IRF alignments, only the domain of interest
603 was used for phylogenetic analysis. Maximum likelihood phylogenetic trees were
604 generated with PhyML using 100 bootstrap replicates. Alignments shown were made in
605 Geneious using Clustal Omega.

606
607 **Nanostring gene expression analysis**
608 A custom codeset targeting 36 genes of interest and 4 housekeeping genes for
609 normalization (Supplementary File S2) was designed by NanoString Technologies
610 (Seattle, WA) for use in nCounter XT CodeSet Gene Expression Assays run on an
611 nCounter SPRINT Profiler (NanoString Technologies). RNA was isolated as it was for
612 qRT-PCR experiments, and hybridized to probes according to the manufacturer's
613 protocol using 50ng/µL of total RNA. Quality control, data normalization, and
614 visualization was performed in nSolver 4.0 analysis software (NanoString Technologies)
615 according to the manufacturer's protocol.
616
617 **Mammalian cell immunofluorescence and confocal microscopy**
618 Glass coverslips were seeded with 293T cells and grown to ~50% confluency.
619 Cells were transfected for 24-48 hours with a total of 1.25 µg of DNA and 3 µL
620 Lipofectamine 2000. Each well contained the following: pcDNA4-STING (10 ng),
621 pEGFP-LC3 (5 ng) and either empty vector or pcDNA4 with the indicated cyclic-
622 dinucleotide synthase (1,235 ng). Cells were washed once in PBS, fixed for 15 minutes
623 in 4% paraformaldehyde, washed once in PBS, and permeabilized for 5 minutes in
624 0.5% saponin in PBS. Cells were then washed once in PBS, and treated with 0.1%
625 sodium borohydride/0.1% saponin/PBS for 5 – 10 minutes in order to consume any
626 remaining paraformaldehyde. Cells were then washed 3 times in PBS, and blocked with
627 blocking buffer (1% BSA/0.1% saponin/PBS) for 45 minutes. Cells were then incubated
628 HA antibody (1:200 dilution, Sigma 11867423001 rat IgG from Roche) in blocking buffer
629 for one hour and washed 3 times in PBS. Each well was then incubated with 0.1%
630 saponin/PBS and secondary antibody (1:500 dilution, Jackson ImmunoResearch, Cy3
631 affinipure donkey anti-rat IgG, 712-165-153) for 45 minutes. Finally, cells were washed
632 3 times in PBS, mounted using VectaShield with DAPI, and dried overnight. Images
633 were acquired using a Zeiss LSM 780 NLO AxioExaminer.
634
635 **Acknowledgements**
636 We are especially grateful to Mark Q. Martindale and Miguel Salinas-Saavedra
637 for *N. vectensis* animals and training. We also thank Matt Gibson for sharing shRNA
638 protocols, and Thomas Gilmore for the anti-nvNF-κB antibody. We thank members of
639 the Vance and Barton labs for discussions, and Arielle Woznica for comments on the
640 manuscript. This work used the Functional Genomic Laboratory and Vincent J. Coates
641 Genomics Sequencing Laboratory at UC Berkeley, supported by NIH S10 OD018174
642 Instrumentation Grant. Confocal imaging experiments were conducted at the CRL
643 Molecular Imaging Center supported by the Gordon and Betty Moore Foundation; we
644 would like to thank Holly Aaron and Feather Ives for training and assistance. REV is an
645 HHMI Investigator and is supported by NIH grants AI0663302, AI075039, and
646 AI155634. SRM is supported by the National Science Foundation Graduate Research
647 Fellowship under Grant Numbers DGE 1106400 and DGE 1752814. B.H. and S.C. were
648 supported by funding from the NIH (R01AI132851 to S.C.), the Chan Zuckerberg
649 Biohub, and the Sangvhi-Agarwal Innovation Award. Any opinions, findings, and
650 conclusions or recommendations expressed in this material are those of the author(s)
651 and do not necessarily reflect the views of the National Science Foundation, HHMI, or
652 the National Institutes of Health.

References

1. J. Ahn, G. N. Barber, STING signaling and host defense against microbial infection. *Exp Mol Med* **51**, 1-10 (2019).
2. A. Ablasser, Z. J. Chen, cGAS in action: Expanding roles in immunity and inflammation. *Science* **363** (2019).
3. L. Sun, J. Wu, F. Du, X. Chen, Z. J. Chen, Cyclic GMP-AMP synthase is a cytosolic DNA sensor that activates the type I interferon pathway. *Science* **339**, 786-791 (2013).
4. P. Gao *et al.*, Cyclic [G(2',5')pA(3',5')p] is the metazoan second messenger produced by DNA-activated cyclic GMP-AMP synthase. *Cell* **153**, 1094-1107 (2013).
5. A. Ablasser *et al.*, cGAS produces a 2'-5'-linked cyclic dinucleotide second messenger that activates STING. *Nature* **498**, 380-384 (2013).
6. E. J. Diner *et al.*, The innate immune DNA sensor cGAS produces a noncanonical cyclic dinucleotide that activates human STING. *Cell reports* **3**, 1355-1361 (2013).
7. X. Zhang *et al.*, Cyclic GMP-AMP containing mixed phosphodiester linkages is an endogenous high-affinity ligand for STING. *Molecular cell* **51**, 226-235 (2013).
8. H. Ishikawa, G. N. Barber, STING is an endoplasmic reticulum adaptor that facilitates innate immune signalling. *Nature* **455**, 674-678 (2008).
9. Y. Tanaka, Z. J. Chen, STING specifies IRF3 phosphorylation by TBK1 in the cytosolic DNA signaling pathway. *Science signaling* **5**, ra20 (2012).
10. S. Liu *et al.*, Phosphorylation of innate immune adaptor proteins MAVS, STING, and TRIF induces IRF3 activation. *Science* **347**, aaa2630 (2015).
11. C. Zhang *et al.*, Structural basis of STING binding with and phosphorylation by TBK1. *Nature* **567**, 394-398 (2019).
12. B. Zhao *et al.*, A conserved PLPLRT/SD motif of STING mediates the recruitment and activation of TBK1. *Nature* **569**, 718-722 (2019).
13. D. B. Stetson, R. Medzhitov, Type I interferons in host defense. *Immunity* **25**, 373-381 (2006).
14. J. W. Schoggins, Interferon-Stimulated Genes: What Do They All Do? *Annu Rev Virol* **6**, 567-584 (2019).
15. T. Abe, G. N. Barber, Cytosolic-DNA-mediated, STING-dependent proinflammatory gene induction necessitates canonical NF-kappaB activation through TBK1. *Journal of virology* **88**, 5328-5341 (2014).
16. H. Chen *et al.*, Activation of STAT6 by STING is critical for antiviral innate immunity. *Cell* **147**, 436-446 (2011).
17. X. Gui *et al.*, Autophagy induction via STING trafficking is a primordial function of the cGAS pathway. *Nature* **567**, 262-266 (2019).
18. T. D. Fischer, C. Wang, B. S. Padman, M. Lazarou, R. J. Youle, STING induces LC3B lipidation onto single-membrane vesicles via the V-ATPase and ATG16L1-WD40 domain. *J Cell Biol* **219** (2020).
19. R. O. Watson, P. S. Manzanillo, J. S. Cox, Extracellular M. tuberculosis DNA targets bacteria for autophagy by activating the host DNA-sensing pathway. *Cell* **150**, 803-815 (2012).

20. R. O. Watson *et al.*, The Cytosolic Sensor cGAS Detects Mycobacterium tuberculosis DNA to Induce Type I Interferons and Activate Autophagy. *Cell host & microbe* **17**, 811-819 (2015).
21. S. Gluck, A. Ablasser, Innate immunosensing of DNA in cellular senescence. *Current opinion in immunology* **56**, 31-36 (2019).
22. M. M. Gaidt *et al.*, The DNA Inflammasome in Human Myeloid Cells Is Initiated by a STING-Cell Death Program Upstream of NLRP3. *Cell* **171**, 1110-1124 e1118 (2017).
23. A. Sze *et al.*, Host restriction factor SAMHD1 limits human T cell leukemia virus type 1 infection of monocytes via STING-mediated apoptosis. *Cell host & microbe* **14**, 422-434 (2013).
24. S. R. Paludan, L. S. Reinert, V. Hornung, DNA-stimulated cell death: implications for host defence, inflammatory diseases and cancer. *Nature reviews. Immunology* **19**, 141-153 (2019).
25. M. F. Gulen *et al.*, Signalling strength determines proapoptotic functions of STING. *Nature communications* **8**, 427 (2017).
26. J. Wu *et al.*, STING-mediated disruption of calcium homeostasis chronically activates ER stress and primes T cell death. *The Journal of experimental medicine* **216**, 867-883 (2019).
27. S. R. Margolis, S. C. Wilson, R. E. Vance, Evolutionary Origins of cGAS-STING Signaling. *Trends Immunol* **38**, 733-743 (2017).
28. D. Cohen *et al.*, Cyclic GMP-AMP signalling protects bacteria against viral infection. *Nature* **574**, 691-695 (2019).
29. B. R. Morehouse *et al.*, STING cyclic dinucleotide sensing originated in bacteria. *Nature* **586**, 429-433 (2020).
30. A. Goto *et al.*, The Kinase IKKbeta Regulates a STING- and NF-kappaB-Dependent Antiviral Response Pathway in Drosophila. *Immunity* **49**, 225-234 e224 (2018).
31. H. Cai *et al.*, 2'3'-cGAMP triggers a STING- and NF-kappaB-dependent broad antiviral response in Drosophila. *Science signaling* **13** (2020).
32. Y. Liu *et al.*, Inflammation-Induced, STING-Dependent Autophagy Restricts Zika Virus Infection in the Drosophila Brain. *Cell host & microbe* **24**, 57-68 e53 (2018).
33. X. Hua *et al.*, Stimulator of interferon genes (STING) provides insect antiviral immunity by promoting Dredd caspase-mediated NF-kappaB activation. *J Biol Chem* **293**, 11878-11890 (2018).
34. M. Martin, A. Hiroyasu, R. M. Guzman, S. A. Roberts, A. G. Goodman, Analysis of Drosophila STING Reveals an Evolutionarily Conserved Antimicrobial Function. *Cell reports* **23**, 3537-3550 e3536 (2018).
35. X. Hua, W. Xu, S. Ma, Q. Xia, STING-dependent autophagy suppresses Nosema bombycis infection in silkworms, Bombyx mori. *Developmental and comparative immunology* **115**, 103862 (2021).
36. N. H. Putnam *et al.*, Sea anemone genome reveals ancestral eumetazoan gene repertoire and genomic organization. *Science* **317**, 86-94 (2007).
37. P. J. Kranzusch *et al.*, Ancient Origin of cGAS-STING Reveals Mechanism of Universal 2',3' cGAMP Signaling. *Molecular cell* **59**, 891-903 (2015).
38. L. H. Yamashiro *et al.*, Interferon-independent STING signaling promotes resistance to HSV-1 in vivo. *Nature communications* **11**, 3382 (2020).

746 39. S. Yum, M. Li, Y. Fang, Z. J. Chen, TBK1 recruitment to STING activates both
747 IRF3 and NF-kappaB that mediate immune defense against tumors and viral
748 infections. *Proceedings of the National Academy of Sciences of the United*
749 *States of America* **118** (2021).
750 40. D. J. Miller *et al.*, The innate immune repertoire in cnidaria--ancestral complexity
751 and stochastic gene loss. *Genome Biol* **8**, R59 (2007).
752 41. A. M. Reitzel, J. C. Sullivan, N. Traylor-Knowles, J. R. Finnerty, Genomic survey
753 of candidate stress-response genes in the estuarine anemone Nematostella
754 vectensis. *Biol Bull* **214**, 233-254 (2008).
755 42. J. J. Brennan *et al.*, Sea anemone model has a single Toll-like receptor that can
756 function in pathogen detection, NF-kappaB signal transduction, and
757 development. *Proceedings of the National Academy of Sciences of the United*
758 *States of America* **114**, E10122-E10131 (2017).
759 43. F. S. Wolenski *et al.*, Characterization of the core elements of the NF-kappaB
760 signaling pathway of the sea anemone Nematostella vectensis. *Molecular and*
761 *cellular biology* **31**, 1076-1087 (2011).
762 44. F. S. Wolenski, C. A. Bradham, J. R. Finnerty, T. D. Gilmore, NF-kappaB is
763 required for cnidocyte development in the sea anemone Nematostella vectensis.
764 *Developmental biology* **373**, 205-215 (2013).
765 45. M. Lewandowska, T. Sharoni, Y. Admoni, R. Aharoni, Y. Moran, Functional
766 characterization of the cnidarian antiviral immune response reveals ancestral
767 complexity. *bioRxiv* 10.1101/2020.11.12.379735, 2020.2011.2012.379735
768 (2020).
769 46. S. Chou *et al.*, Transferred interbacterial antagonism genes augment eukaryotic
770 innate immune function. *Nature* **518**, 98-101 (2015).
771 47. L. G. Rahme *et al.*, Plants and animals share functionally common bacterial
772 virulence factors. *Proceedings of the National Academy of Sciences of the United*
773 *States of America* **97**, 8815-8821 (2000).
774 48. S. Franzenburg *et al.*, MyD88-deficient Hydra reveal an ancient function of TLR
775 signaling in sensing bacterial colonizers. *Proceedings of the National Academy of*
776 *Sciences of the United States of America* **109**, 19374-19379 (2012).
777 49. A. B. Russell *et al.*, Type VI secretion delivers bacteriolytic effectors to target
778 cells. *Nature* **475**, 343-347 (2011).
779 50. B. M. Hayes *et al.*, Ticks Resist Skin Commensals with Immune Factor of
780 Bacterial Origin. *Cell* **183**, 1562-1571 e1512 (2020).
781 51. B. C. Krasity, J. V. Troll, J. P. Weiss, M. J. McFall-Ngai, LBP/BPI proteins and
782 their relatives: conservation over evolution and roles in mutualism. *Biochem Soc*
783 *Trans* **39**, 1039-1044 (2011).
784 52. O. Levy, C. E. Ooi, J. Weiss, R. I. Lehrer, P. Elsbach, Individual and synergistic
785 effects of rabbit granulocyte proteins on Escherichia coli. *J Clin Invest* **94**, 672-
786 682 (1994).
787 53. B. Loh, C. Grant, R. E. Hancock, Use of the fluorescent probe 1-N-
788 phenylnaphthylamine to study the interactions of aminoglycoside antibiotics with
789 the outer membrane of Pseudomonas aeruginosa. *Antimicrob Agents Chemother*
790 **26**, 546-551 (1984).
791 54. P. N. Paradkar, L. Trinidad, R. Voysey, J. B. Duchemin, P. J. Walker, Secreted
792 Vago restricts West Nile virus infection in Culex mosquito cells by activating the

Jak-STAT pathway. *Proceedings of the National Academy of Sciences of the United States of America* **109**, 18915-18920 (2012).

55. T. J. Green, P. Speck, Antiviral Defense and Innate Immune Memory in the Oyster. *Viruses* **10** (2018).
56. A. Woznica *et al.*, STING mediates immune responses in a unicellular choanoflagellate. *bioRxiv* (2021).
57. D. L. Burdette *et al.*, STING is a direct innate immune sensor of cyclic di-GMP. *Nature* **478**, 515-518 (2011).
58. D. Zhu *et al.*, Structural biochemistry of a Vibrio cholerae dinucleotide cyclase reveals cyclase activity regulation by folates. *Molecular cell* **55**, 931-937 (2014).
59. D. J. Stefanik, L. E. Friedman, J. R. Finnerty, Collecting, rearing, spawning and inducing regeneration of the starlet sea anemone, Nematostella vectensis. *Nat Protoc* **8**, 916-923 (2013).
60. A. Karabulut, S. He, C. Y. Chen, S. A. McKinney, M. C. Gibson, Electroporation of short hairpin RNAs for rapid and efficient gene knockdown in the starlet sea anemone, Nematostella vectensis. *Developmental biology* **448**, 7-15 (2019).
61. M. J. Layden, E. Rottinger, F. S. Wolenski, T. D. Gilmore, M. Q. Martindale, Microinjection of mRNA or morpholinos for reverse genetic analysis in the starlet sea anemone, Nematostella vectensis. *Nat Protoc* **8**, 924-934 (2013).
62. F. S. Wolenski, M. J. Layden, M. Q. Martindale, T. D. Gilmore, J. R. Finnerty, Characterizing the spatiotemporal expression of RNAs and proteins in the starlet sea anemone, Nematostella vectensis. *Nat Protoc* **8**, 900-915 (2013).
63. D. I. Kotov, T. Pengo, J. S. Mitchell, M. J. Gastinger, M. K. Jenkins, Chrysalis: A New Method for High-Throughput Histo-Cytometry Analysis of Images and Movies. *Journal of immunology* **202**, 300-308 (2019).

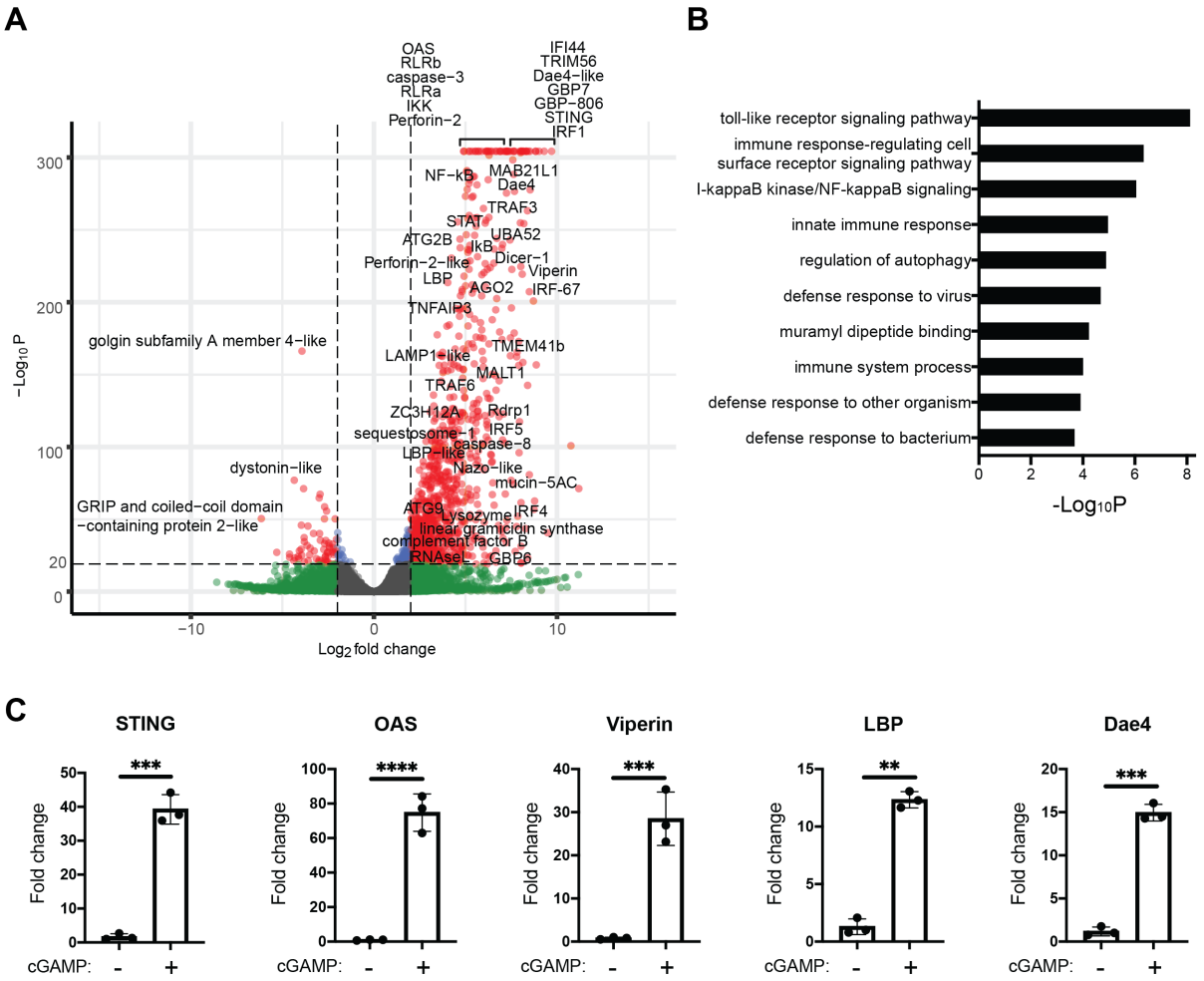

Figure 1: 2'3'-cGAMP induces many putative immune genes in *Nematostella vectensis*

A) Volcano plot showing differential gene expression (DE) in *N. vectensis* polyps untreated vs. treated with 2'3'-cGAMP for 24 hours. A positive fold-change indicates higher expression in polyps treated with 2'3'-cGAMP. Genes of interest with homologs known to be involved in immunity in other organisms are labeled.

B) Breakdown of DE genes into categories based on known GO terms. Gene set enrichment analysis shows a clear enrichment of GO terms associated with immunity.

C) qRT-PCR measuring genes of interest in 48-hour-old *N. vectensis* embryos untreated or treated with 2'3'-cGAMP for 4 hours. Fold changes were calculated relative to untreated as $2^{-\Delta\Delta Ct}$ and each point represents one biological replicate. Unpaired t test performed on ΔΔCt before log transformation. *$p \leq 0.05$; **$p \leq 0.01$; ***$p \leq 0.001$; ****$p \leq 0.0001$.

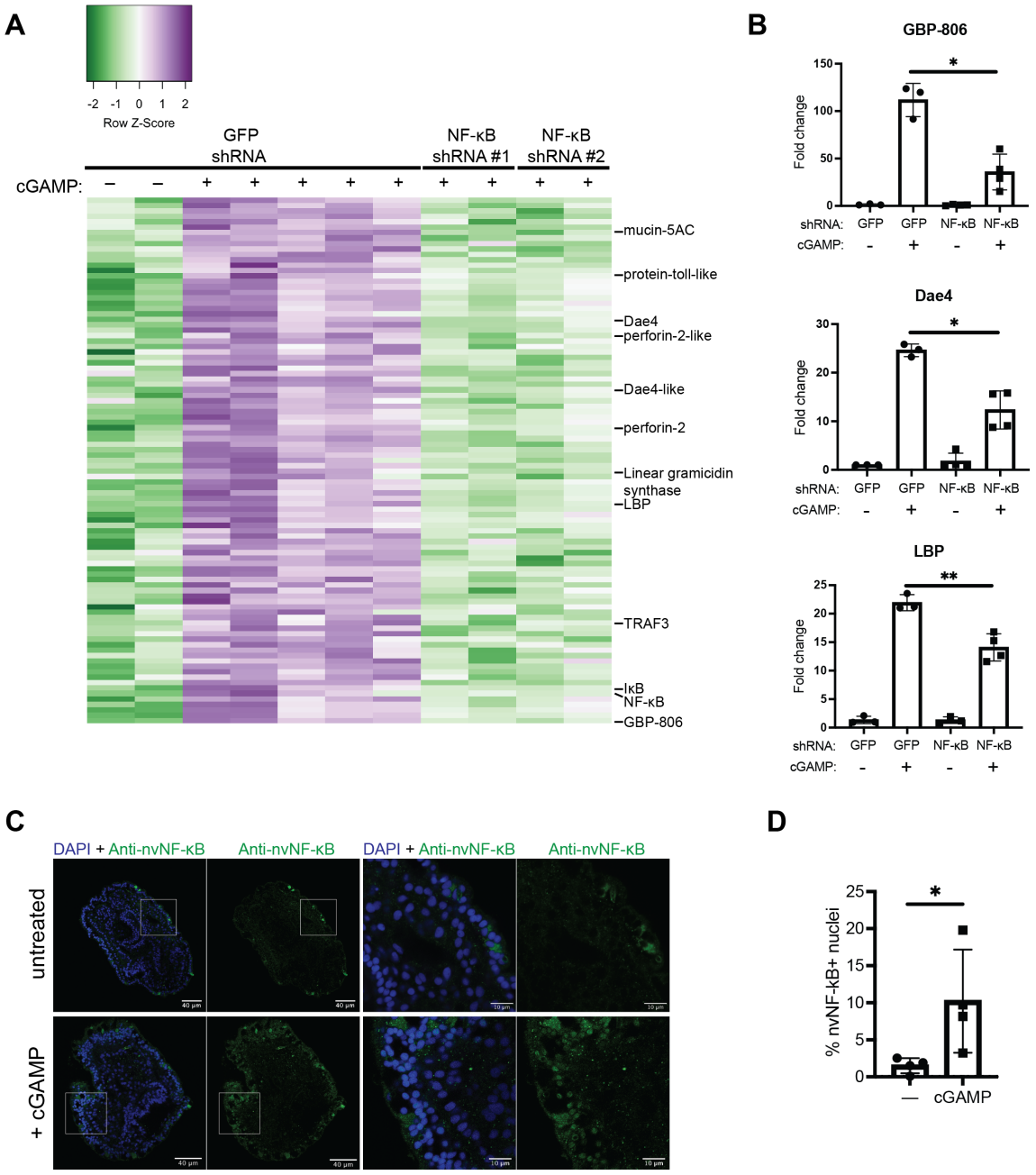

Figure 2: The induction of many anti-bacterial genes by 2'3'-cGAMP is nvNF-κB dependent

A) Heatmap showing all genes that are significantly (padj < 0.05, $\log_2$FC<-1) downregulated in 2'3'-cGAMP -treated embryos microinjected with NF-κB shRNA vs. GFP shRNA. Genes with predicted antibacterial function are labeled

B) qRT-PCR of antibacterial genes in nvNF-kB shRNA or control GFP shRNA treated samples after induction by 2'3'-cGAMP. Fold change was calculated relative to untreated, GFP shRNA injected as $2^{-\Delta\Delta Ct}$ and each point represents

one biological replicate. Unpaired t test performed on ΔΔCt before log transformation. *$p \leq 0.05$; **$p \leq 0.01$.

C) Whole mount immunofluorescence of polyps stained with anti-nvNF-κB antiserum. Right two panels are enlargements of the boxed regions indicated in the left two panels..

D) Quantification of cells with nuclear localization of nvNF-kB after treatment with cGAMP (representative images shown in C). Each point represents a single polyp, in which at least 1500 cells were analyzed. Statistical analysis was performed by unpaired t test; *$p = 0.0481$.

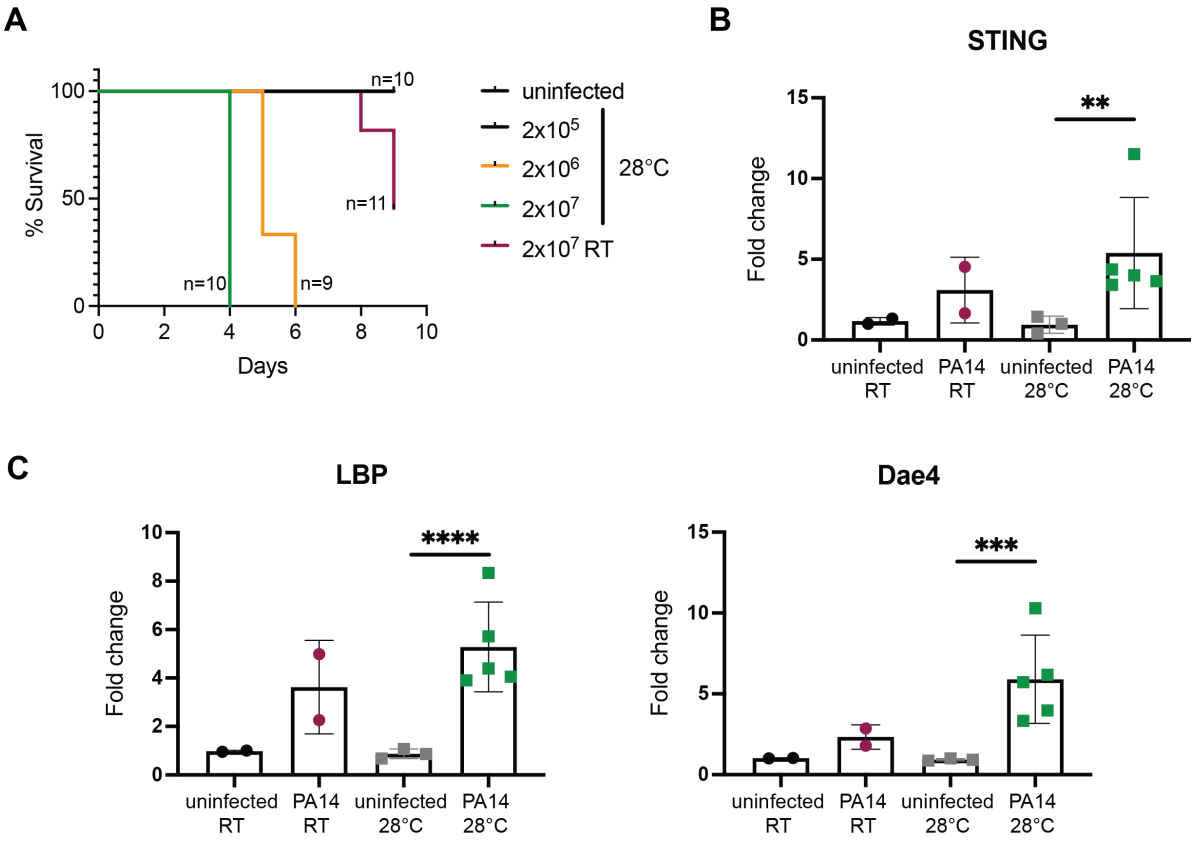

Figure 3: *Pseudomonas aeruginosa* infection induces putative anti-bacterial genes

A) Survival curves of *N. vectensis* polyps infected with *P. aeruginosa* at indicated dose and temperature.

B+C) qRT-PCR of nvSTING (B) or putative antibacterial genes (C) assayed at 48 hours post *Pa* infection ($2x10^7$ CFU/ml). Each point represents one biological replicate; unpaired t test performed on ΔΔCt before log transformation. $^{**}p \leq 0.01$; $^{***}p \leq 0.001$; $^{****}p \leq 0.0001$.

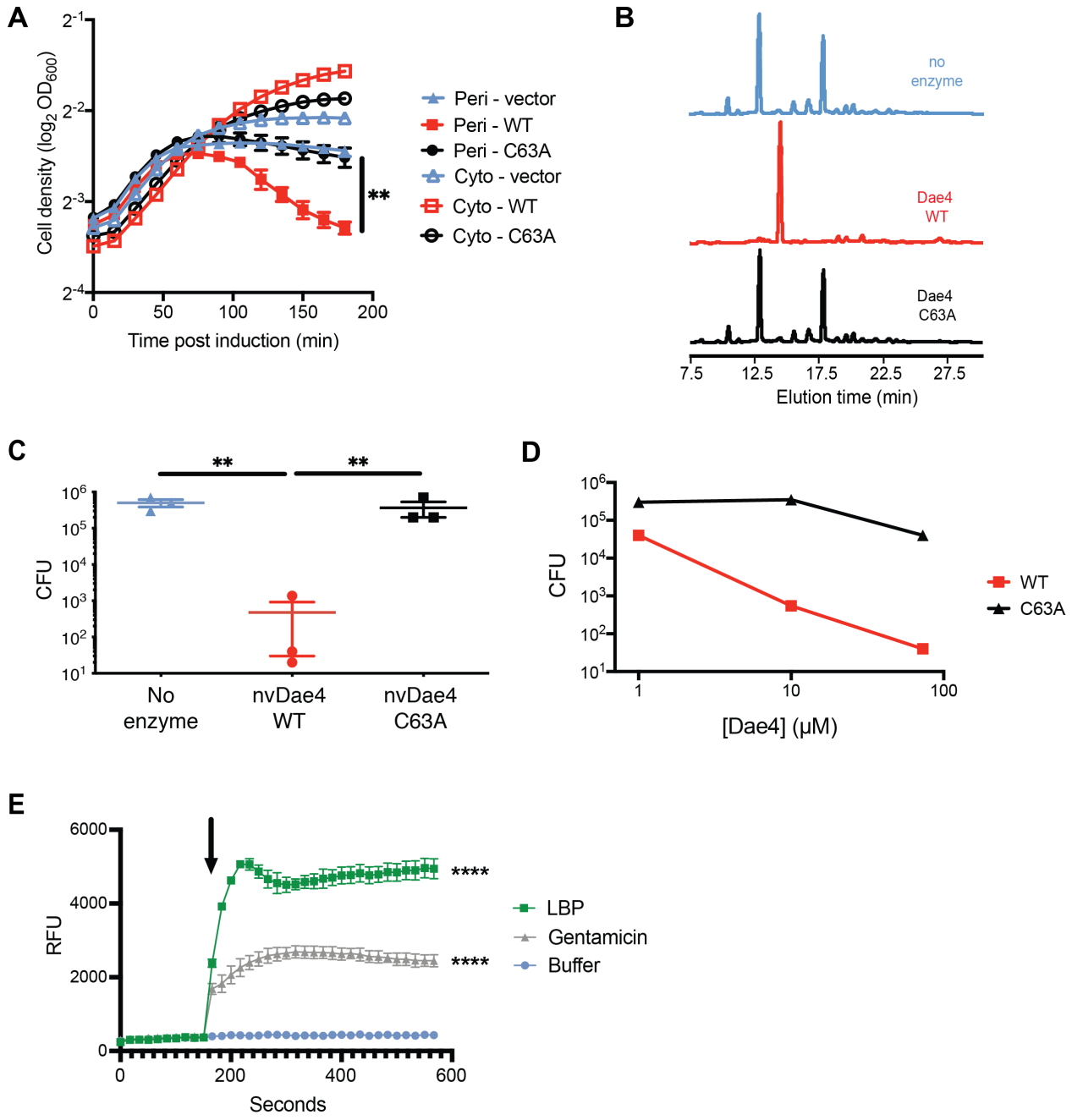

Figure 4: 2'3'-cGAMP induced, nvNF-κB-dependent proteins have anti-bacterial activity

A) Growth of *E. coli* expressing either periplasmic (Peri-) or cytosolic (Cyto-) nvDae4 (WT or C63A) induced with 250μM IPTG. Error bars +/- SD; n=3. Unpaired t test; **p = 0.0063.

B) Partial HPLC chromatograms of *E. coli* peptidoglycan sacculi after overnight incubation with buffer only (no enzyme), or 1 μM nvDae4 WT or C63A enzyme.

C) *Bacillus subtilis* CFU after 2 hour incubation with buffer alone, nvDae4 WT or catalytic mutant C63A (25 μM). Error bars +/- SEM; n=3. Unpaired t test performed on log-tranformed values; **p ≤ 0.01.

D) Dose dependent killing of *B. subtilis* by WT nvDae4 enzyme (same assay as in C).
E) Fluorescence of *P. aeruginosa* (uptake of NPN) after treatment with nvLBP (4.5 μM) or gentamicin (20 μg/mL). Arrow indicates time gentamicin or nvLBP was added. Unpaired t test ; ****$p \leq 0.0001$.

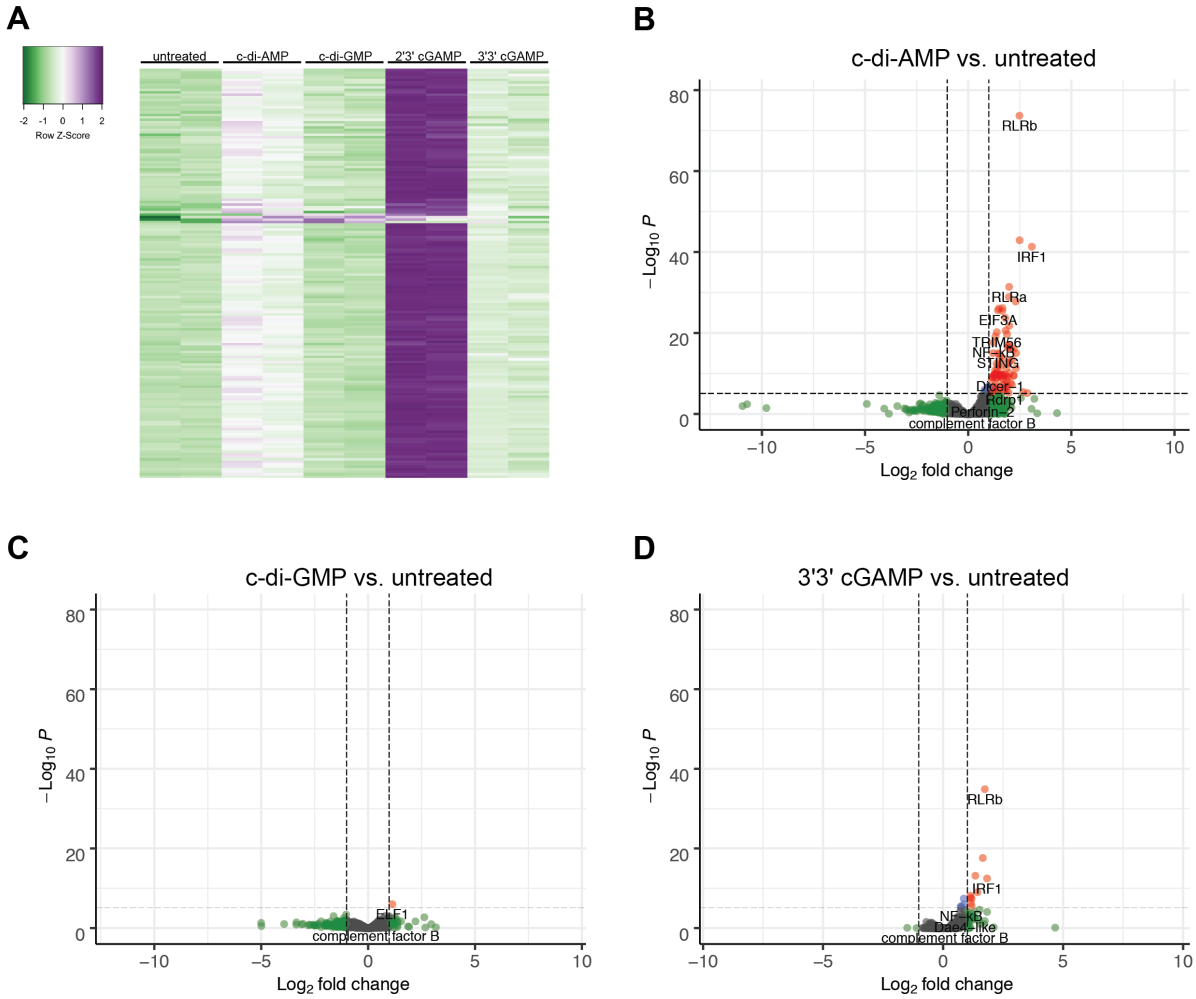

Figure S1: Treatment with other CDNs leads to some gene induction

A) Heatmap showing differentially expressed genes in response to c-di-AMP, c-di-GMP, and 3'3'-cGAMP. Almost all of these are also significantly induced by 2'3'-cGAMP.

B-D) Volcano plots of differential gene expression in *N. vectensis* polyps untreated vs. treated with cyclic-di-AMP (B), cyclic-di-GMP (C) and 3'3'-cGAMP (D) for 24 hours.

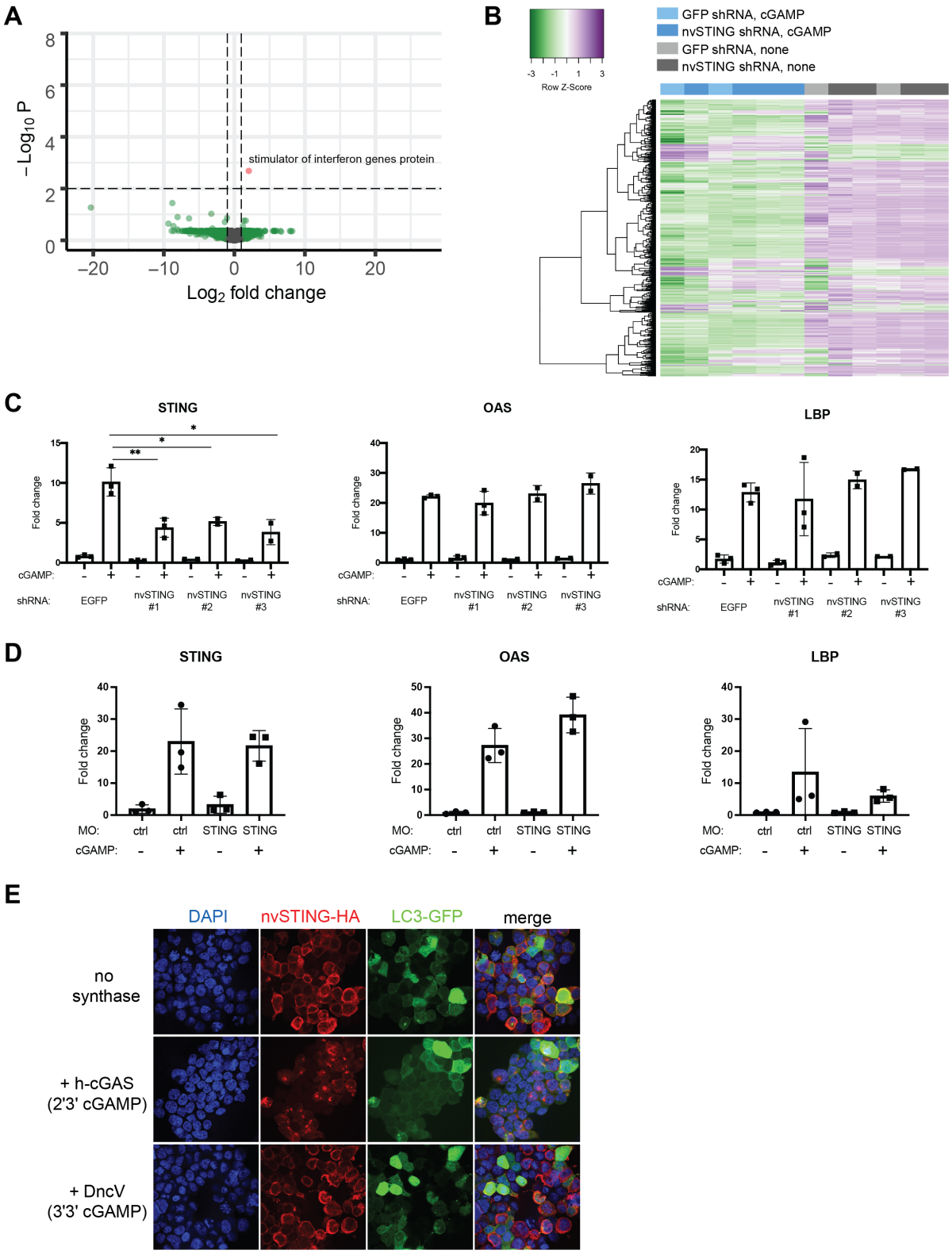
A
stimulator of interferon genes protein
$-\text{Log}_{10}$ P
Log_2 fold change
B
Row Z-Score
GFP shRNA, cGAMP
nvSTING shRNA, cGAMP
GFP shRNA, none
nvSTING shRNA, none
C
STING
OAS
LBP
Fold change
cGAMP:
shRNA:
EGFP
nvSTING #1
nvSTING #2
nvSTING #3
D
STING
OAS
LBP
Fold change
MO:
ctrl
STING
cGAMP:
E
DAPI
nvSTING-HA
LC3-GFP
merge
no synthase
+ h-cGAS (2'3' cGAMP)
+ DncV (3'3' cGAMP)

Figure S2: nvSTING knockdown does not impact the induction of genes by 2'3'-cGAMP

A) Volcano plot showing differential gene expression in 48 hour embryos treated with 2'3'-cGAMP that were injected with GFP shRNA or nvSTING shRNA. Positive fold-change indicates higher expression in GFP shRNA injected embryos.
B) Clustered heatmap showing the expression of the top 1000 varied genes by RNA-Seq between embryos injected with either GFP or nvSTING shRNA and either untreated or treated with 2'3'-cGAMP.
C) Fold change of nvSTING, nvOAS, and nvLBP assayed by Nanostring from experiments using 3 different shRNAs to knock down nvSTING expression.
D) qRT-qPCR measuring genes of interest in 48-hour-old embryos injected with a control (ctrl) or nvSTING translation-inhibiting morpholino (MO) and treated with 2'3'-cGAMP. Fold changes were calculated as $2^{-\Delta\Delta Ct}$ and each point represents one biological replicate. Unpaired t test performed on ΔΔCt before log transformation; no significant differences.
E) Immunofluorescence images of 293T cells transfected with plasmids encoding nvSTING-HA, LC3-GFP, and either empty vector, human cGAS or *V. cholera* DncV. Human cGAS is activated by the transfected DNA to produce 2'3'-cGAMP, and DncV, which produces 3'3'-cGAMP, is constitutively active in 293T cells.

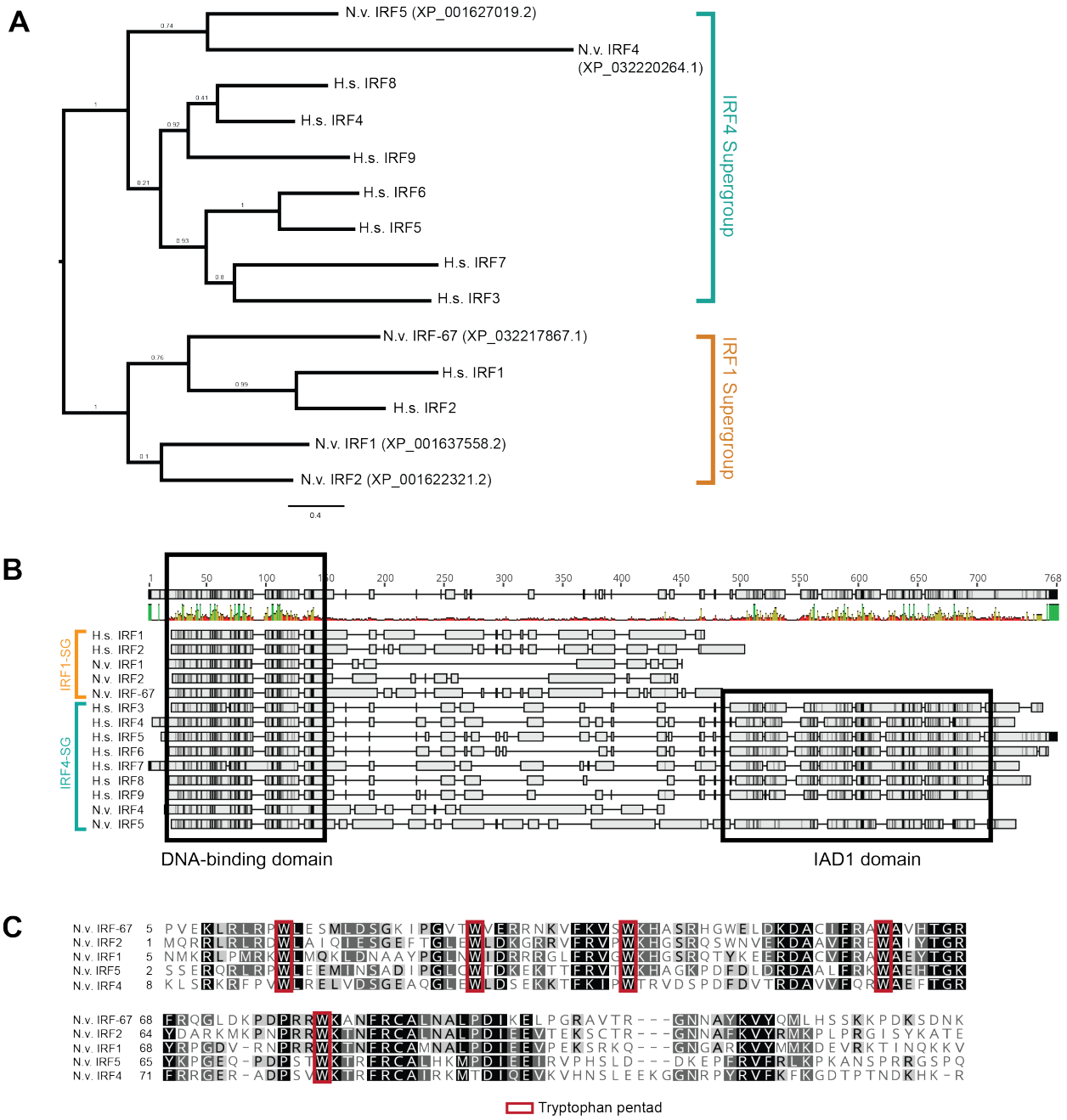

Figure S3: Phylogenetic study of *N. vectensis* IRFs

A) Phylogenetic tree of all human and *N. vectensis* IRF proteins. 3 nvIRFs cluster with members of the human IRF1 supergroup, while the other 2 nvIRFs cluster with the IRF4 supergroup.

B) Full protein alignment of sequences in A). The DNA-binding domain is highly conserved between all *N. vectensis* and human IRFs. Only nvIRF5 contains an IAD1 domain.

C) Alignment of all nvIRF DNA-binding domains with conserved tryptophan pentad outlined in red

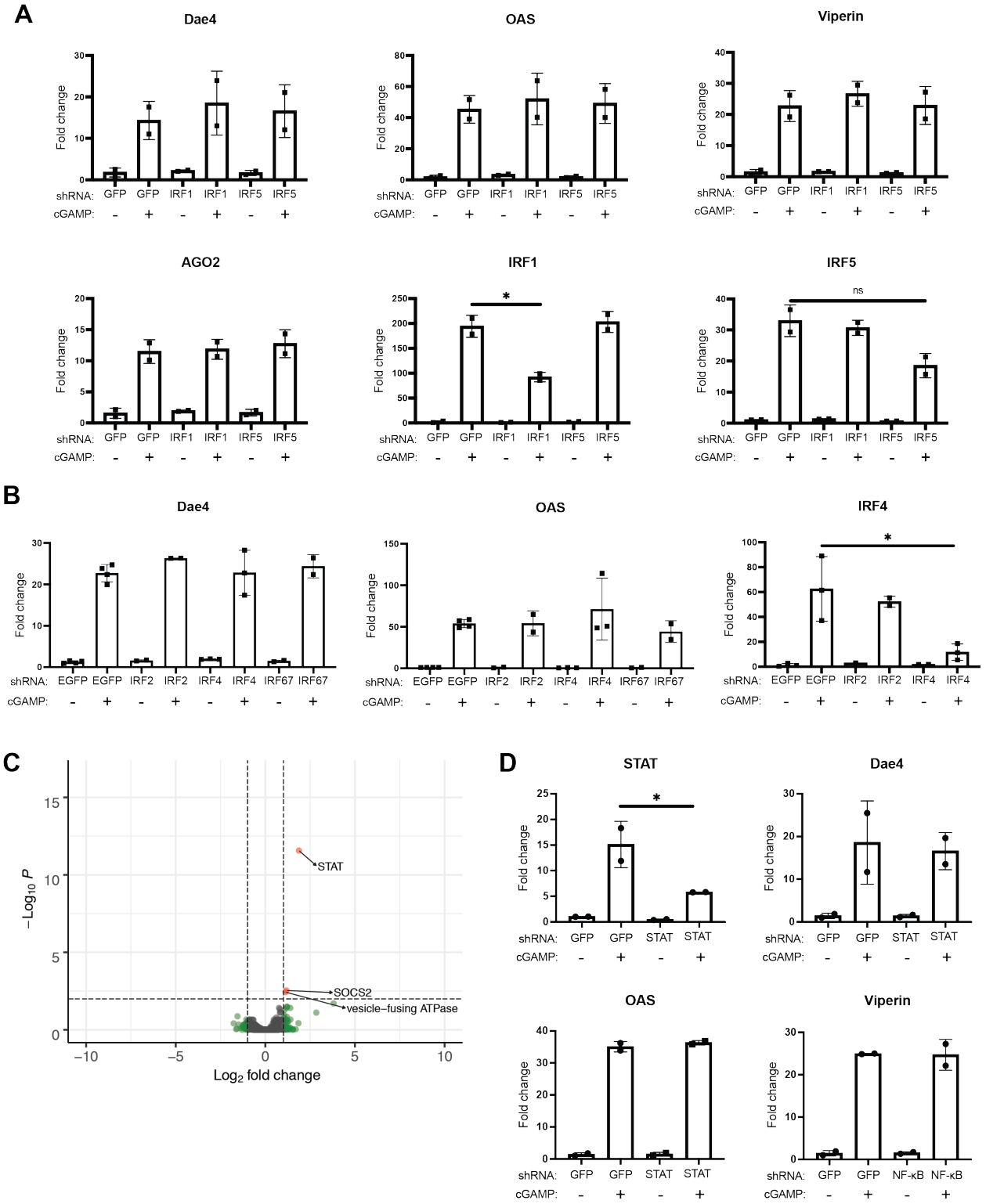
A
Dae4
OAS
Viperin
AGO2
IRF1
IRF5
Fold change
shRNA: GFP GFP IRF1 IRF1 IRF5 IRF5
cGAMP: - + - + - +
*
ns
B
Dae4
OAS
IRF4
shRNA: EGFP EGFP IRF2 IRF2 IRF4 IRF4 IRF67 IRF67
C
STAT
SOCS2
vesicle–fusing ATPase
−Log10 P
Log2 fold change
D
STAT
Dae4
OAS
Viperin
shRNA: GFP GFP STAT STAT
shRNA: GFP GFP NF-κB NF-κB

Figure S4: Knockdowns of nvIRFs or nvSTAT have no effect on 2'3'-cGAMP-induced gene expression

A) Fold changes in gene expression as determined by Nanostring in embryos microinjected with shRNAs targeting EGFP, nvIRF1, or nvIRF5 either untreated or treated with 2'3'-cGAMP.
B) Fold changes in gene expression as determined by qRT-PCR in samples microinjected with shRNAs targeting EGFP, nvIRF2, nvIRF-67, or nvIRF4 either untreated or treated with 2'3'-cGAMP. Note that IRF2 is not induced by cGAMP and was mostly undetected in all samples; therefore it is possible that the knockdowns were unsuccessful.
C) Volcano plot showing differential gene expression as determined by RNA-Seq in 48 hour embryos treated with 2’3’-cGAMP that were injected with GFP shRNA or nvSTAT shRNA. Positive fold-change indicates higher expression in GFP shRNA injected embryos. The GFP shRNA samples here are the same as those shown in Figure 2A.
D) Fold changes in gene expression as determined by Nanostring in embryos microinjected with shRNAs targeting EGFP or nvSTAT either untreated or treated with 2'3'-cGAMP.

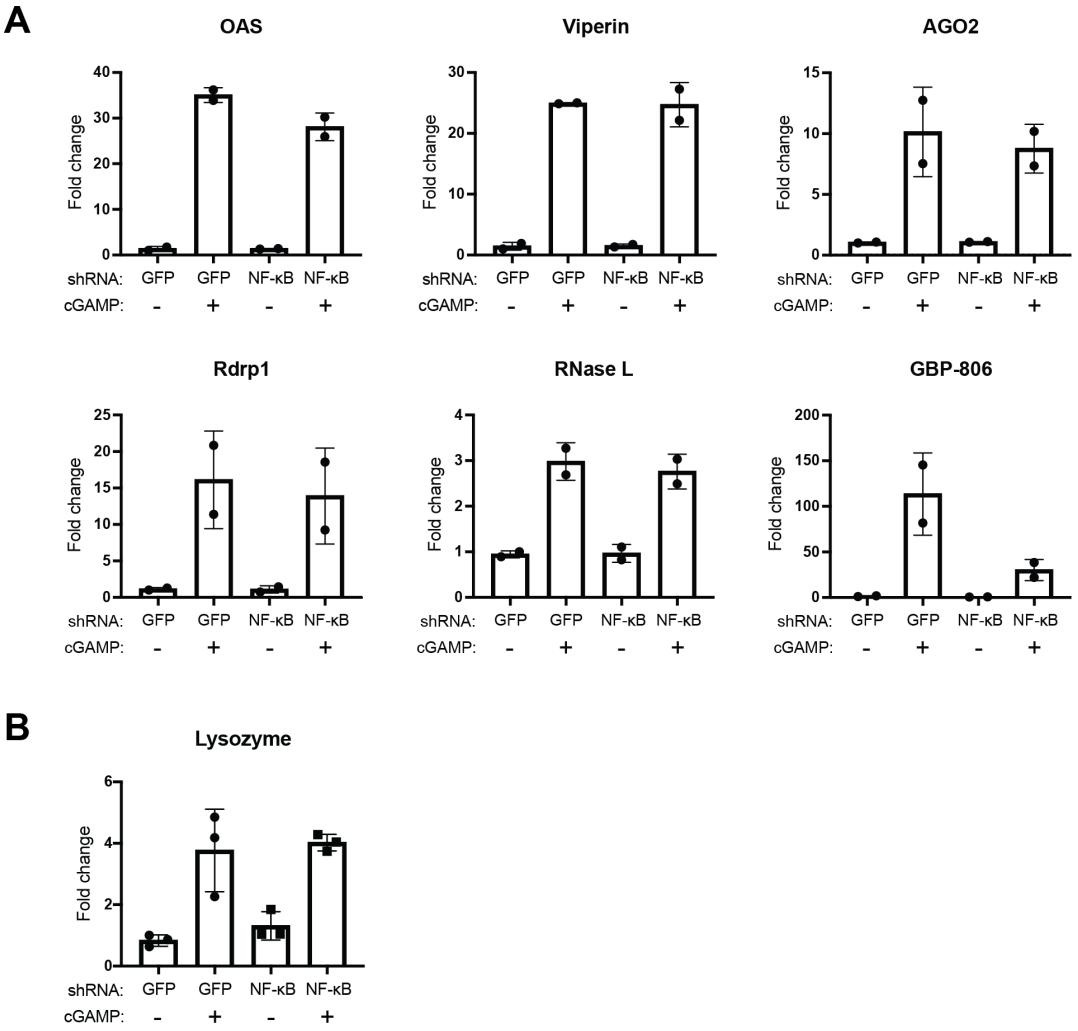

Figure S5: Anti-viral gene induction is not dependent on nvNF-κB

A) Fold changes in gene expression as determined by Nanostring in embryos microinjected with shRNAs targeting EGFP or nvNF-κB, either untreated or treated with 2'3'-cGAMP. The GFP shRNA samples here are the same as those shown in Figure S4. GBP-806 expression included to show anti-bacterial gene induction is lower in these samples.

B) Fold changes in nvLysozyme expression as determined by qRT-PCR in embryos microinjected with shRNAs targeting EGFP or nvNF-κB, either untreated or treated with 2'3'-cGAMP.

A+B) No significant differences in gene expression are observed between any cGAMP treated samples.

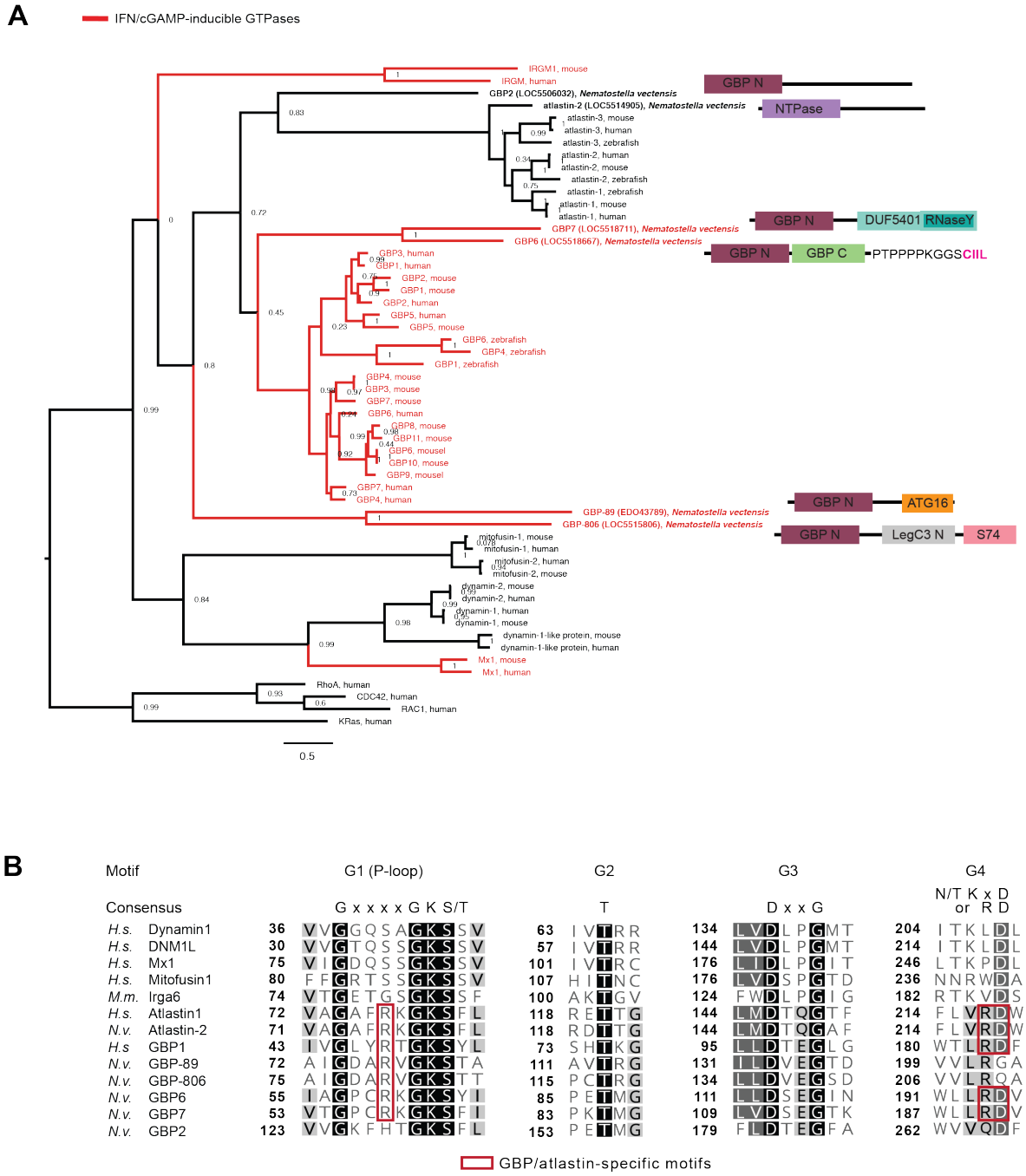

Figure S6: Phylogenetic study of *N. vectensis* GBPs

A) Phylogenetic tree of mammalian GTPases and putative *N. vectensis* GBPs made with the full protein sequences. Branches with mammalian interferon-induced GTPases and cGAMP-induced *N. vectensis* GBPs are colored red; these tend to cluster together. Domain structures of *N. vectensis* GBPs are displayed.

B) Alignment of the GTPase domains of all *N. vectensis* GBPs and select mammalian GTPase. Conserved GBP and atlastin specific residues are highlighted in red.

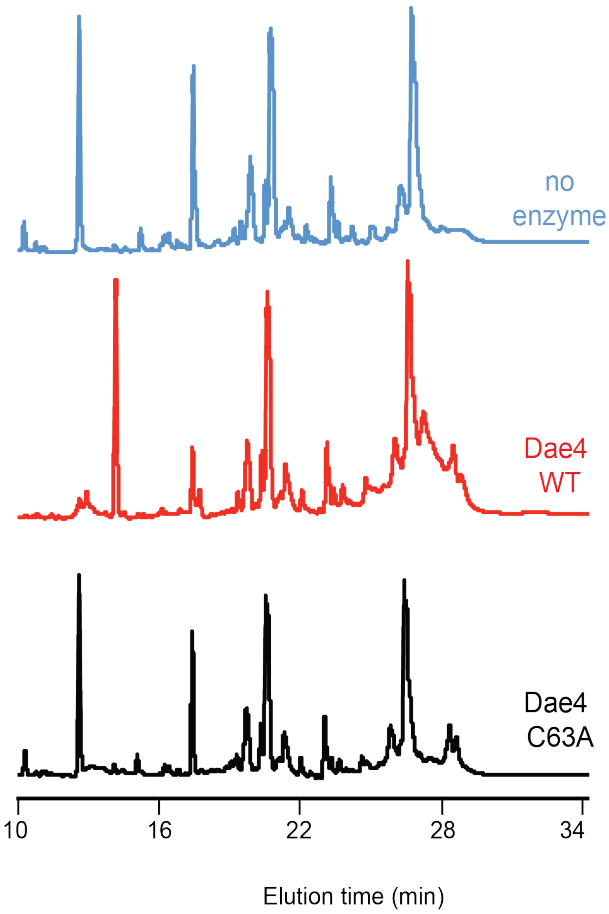

Figure S7: nvDae4 cleaves peptidoglycan from Gram-positive bacteria. Partial HPLC chromatograms of *Staphylococcus epidermis* peptidoglycan sacculi products resulting from incubation with buffer only (no enzyme), or 1 μM nvDae4 WT or C63A enzyme.

Table S1: Cnidarian-specific genes that are induced by 2'3'-cGAMP in an nvNF-κB-dependent manner

NCBI Gene ID	Domains	Only in Cnidaria?	Only in Anthozoa?	Homolog found in immune cells in *Stylophora pistillata(1)*?
5501851	none	yes	yes	no
5504224	MDN1 super family	yes	yes	no
5516219	none	yes	yes	no
5516219	none	yes	yes	no
5518710	none	yes	yes	no
116603205	none	yes	yes	No homolog in *Stylophora pistillata*
116603727	none	yes	yes	No homolog in *Stylophora pistillata*
116604070	none	yes; except Bacillus spore coat proteins	yes; except Bacillus spore coat proteins	No homolog in *Stylophora pistillata*
116604505	none	yes	yes	No homolog in *Stylophora pistillata*
116612667	none	yes	yes	no
116613998	none	yes	yes	no
116616875	none	yes	yes; similar to 116620239	No homolog in *Stylophora pistillata*
116619128	none	yes	no	yes
116620239	none	yes	yes; similar to 116616875	No homolog in *Stylophora pistillata*

1. S. Levy *et al.*, A stony coral cell atlas illuminates the molecular and cellular basis of coral symbiosis, calcification, and immunity. *Cell* 10.1016/j.cell.2021.04.005 (2021).